Gross External Damages of Water Pollution in the United States

David A. Keiser, Tihitina Andarge, Mohammad Mainul Hoque, Yongjie Ji, Catherine L. Kling, Daniel J. Phaneuf, Nilesh Shinde, and Yau-Huo Shr*

March 19, 2025

Abstract

This paper provides the first estimates of the Gross External Damages (GED) of water pollution in the US. We focus on nutrient pollution, which is responsible for most surface water impairments. To measure marginal damages, or implicit prices, we model the fate and transport of pollution through 2.7 million river segments. Marginal damages are largest near bodies of water and population centers. Twenty percent of the nation's watersheds are responsible for eighty percent of damages. Average marginal damages exceed $338/kg, which exceeds fertilizer prices, a common source of pollution, by two orders of magnitude. Total damages are approximately $140B annually.

JEL Codes: H23, Q51, Q52, Q53, Q56

*Corresponding author: Keiser, e-mail: dkeiser@umass.edu. We thank Joel Corona, Eli Fenichel, Julie Hewitt, Robert Mendelsohn, Nicholas Muller, Sheila Olmstead, Ivan Rudik and participants at the 2020 AAEA meetings, 2021 AERE meetings, 2022 EAERE meetings, 2023 Environmental and Energy Economics workshop at UT Austin, the Social Cost of Water Pollution Workshop, Cornell, Penn State, UC Berkeley, UC San Diego, the University of Alaska-Anchorage, the University of Florida, the University of Minnesota, Wisconsin, and Yale for helpful comments and discussions. We thank the U.S. Department of Agriculture, National Institute of Food and Agriculture, Agriculture and Food Research Initiative (grant numbers 2022-67023-36377 and 2019-67023-29637), the U.S. Environmental Protection Agency's Science to Achieve Program (grant numbers R84065 and R836166), Iowa DNR, National Institutes of Health (grant number R01AG079914A), the Center for Agricultural and Rural Development at Iowa State, and the Cornell Atkinson Center for funding. The content is solely the responsibility of the authors and does not necessarily represent the official views of the National Institutes of Health. Further, the findings and conclusions in this article have not been formally disseminated by the U. S. Department of Agriculture and should not be construed to represent any agency determination or policy.

1 Introduction

Gross Domestic Product is one of the most common measures of economic activity. Its acronym, GDP, features prominently in mainstream media and is memorized by scores of introductory economics students each year. It also serves as one of the most important indicators for setting domestic and global policies. Yet, important shortcomings exist. One widely known limitation is that GDP performs poorly in measuring (or omits entirely) the value of essential environmental goods and services.

The concept of augmenting national economic accounts to include GDP-equivalent measures of the environment is not new. At least fifty years ago, Nordhaus and Tobin (1973) illustrated how one could adjust common measures of economic growth for important non-market goods and services. For decades since, economists have proposed approaches to incorporate "nature's numbers" into estimates of economic activity (NRC, 1999). Implementation of these efforts has begun in earnest on the international stage. For example the World Bank estimates that the value of renewable natural capital per capita has fallen by 20 percent since 1995 (The World Bank, 2024). Commitments by the US government to estimate these values have significantly lagged behind those of other countries, although in January 2023, the Biden White House reignited US-based efforts by directing a fifteen year, multi-agency plan to finally "put nature on the nation's balance sheet" (The White House, 2023; Bagstad et al., 2021). In the absence of governmental accounts, some researchers have produced national-level statistics on the gross external damages of air and climate pollution in the US (Muller et al., 2011; Tschofen et al., 2019; Cropper and Park, 2023). A critical roadblock has been the absence of other estimates of nature's "prices" (Arrow et al., 2012; Fenichel et al., 2016). This paper provides the first estimates of the marginal damages (i.e., implicit prices) of US water pollution and uses them to estimate Gross External Damages (GED), the GDP-equivalent measure of the damages from water pollution.

A central innovation of this paper is a new national integrated assessment model (IAM) of water pollution. This model, which we term HydroEcon, links sources of pollution to impacts on individual water resources throughout the nation and ultimately to households and economic uses of these resources. To develop this model, we first propose a framework for constructing the social cost of water pollution while incorporating the spatial variability of damages. This first step is important, as it guides our interpretation of how to aggregate damages across space and uses of water resources. Like air, but unlike carbon, the damages from water pollution depend critically on the location of emissions (Keiser and Muller, 2017).

In moving from theory to measurement, we first model the flow and fate of water pollution throughout the contiguous US using the National Hydrography Database (NHD) Plus V2 and the US Geological Survey's (USGS) SPAtially-Referenced Regression On Watershed attributes (SPARROW) model. The NHDPlusV2 provides a comprehensive mapping of rivers, streams, lakes, and other waterbodies in the US.[1] Our model uses approximately 2.7 million river and stream segments and over 350,000 lakes that we observe from this database. We then link these water features with SPARROW to model baseline and simulated changes in nutrient pollution levels (nitrogen and phosphorus). SPARROW is a state-of-the-art hydrological model that the USGS has refined over two and a half decades (Smith et al., 1997). It provides highly granular information on long-run average concentrations of nutrient pollution, its flow and fate, and the sources of nutrient pollution. Throughout the paper, we often summarize water pollution data at the watershed level. We define a watershed in this paper as an 8-digit hydrologic unit code (HUC). There are approximately 2,100 8-digit HUCs in the US, or roughly two-thirds of the number of US counties. We focus on nutrient pollution, as it "is one of America's most widespread, costly, and challenging environmental problems" (USEPA, 2024). The effects of excess nutrients are marked by thick, odorous, and potentially harmful algal mats, as well as decreased clarity and ecological integrity.

Next, we link our hydrological system to people. We focus on four main areas of impact: water-based recreation, housing markets, drinking water treatment, and climate change. Prior literature has established these categories as the most likely human uses affected by water pollution in the US (Freeman, 1982; Dodds et al., 2009; Egan et al., 2009; Keiser, 2019; Downing et al., 2021; Mamun et al., 2023). To estimate localized damages, our model utilizes the count of housing units and assessed values from Core Logic's parcel level data file, census tract information on socio-demographics from the US Census, county-level recreational data from the US Department of Agriculture's (USDA) National Survey on Recreation and the Environment, and drinking water intake and service location data from the US Environmental Protection Agency (USEPA). To estimate climate damages, we rely on water resource features that are important for determining climate impacts (i.e., lake size and pollution concentrations). We then develop valuation functions for each of the four main categories. These functions provide estimates of the economic damages that arise from changes in pollution concentrations. We estimate some of these empirical relationships within the paper and borrow from decades of research to establish others.

[1]This mapping effort has been supported by the US Environmental Protection Agency and USGS since the early 2000s and serves as the leading source for information on hydrologic networks for economic analyses (e.g., Keiser and Shapiro (2019)).

Our analysis proceeds by simulating how baseline surface water quality concentrations change with a marginal change in pollution emissions at nearly all of our 2.7 million river segments.[2] We conduct this simulation one river segment at a time. We track how marginal load changes impact local and downstream water quality. We then link these changes in water quality to changes in economic behavior and value. Using this procedure, we recover total marginal damages, or implicit prices, of pollution for each watershed. We combine this information with data on total loads by nutrient pollution sources to estimate total GED. This step allows us to assign marginal and total damages to agricultural, urban, and municipal sources. While we estimate separate damages for phosphorus and nitrogen pollution depending on the use category that they likely impact, we report most of our statistics as marginal damages of nutrient pollution. These nutrients are highly correlated, and it is often difficult to tease out their separate impacts on aquatic systems and economic uses.

Our results suggest large and important impacts of nutrient pollution across the US. Social costs are higher near bodies of water and in urban areas, reflecting the importance of population in determining total damages. Average marginal damages in the Northeast and West are highest with values of \$822 and \$1,019 per kg of nutrient pollution respectively. In the South and Midwest, average marginal damages are significantly lower (\$221/kg and \$161/kg respectively) than those in other areas of the country, reflecting to some extent lower population numbers. GED reflects both prices and quantity. Though marginal damages in the Northeast are higher than the South and Midwest, GED is lowest in the Northeast due to lower levels of emissions.

An important aspect of nutrient pollution is that it flows downstream over large distances. We find that localized damages account for approximately 80% of damages[3], whereas the remaining 20% arises from downstream impacts. We also find that approximately 20% of damages are exported to downstream states, highlighting the importance of cross-boundary pollution. We find other notable spatial patterns in damages. Twenty percent of watersheds in the US are responsible for approximately 80% of GED. These findings highlight particular locations where abatement efforts would likely have the highest societal returns.

We find that water-based recreation reflects the largest share of economic damages. Marginal damages for recreation are at least an order of magnitude larger (\$319/kg) than those of other categories, including housing (\$7.5/kg), drinking water treatment (\$0.02/kg),

[2]As we explain in Section 3, we restrict this procedure to the 2.5 million river segments that fall entirely within a HUC8 to simplify estimates of watershed-specific marginal damages.

[3]We refer to localized damages as those that occur within the same watershed as the source of pollution.

and climate change ($11.4/kg). Prior work has suggested a large role for water-based recreation in overall water pollution damages. Given the public good nature of the problem, damages are also highly correlated with population. Two-thirds of the U.S. population participates in water-based recreational use (Keiser, 2019). However, only around 800 drinking water treatment plants face potential nutrient pollution issues and only 3% of the population lives in a home within 1/2 km of a lake. As a global pollution issue, climate damages are not dependent on local population characteristics, so they are our only category of damages that do not scale with local population numbers.

Non-point sources of nutrient pollution represent the overwhelming share of total pollution loads in U.S. waterways. In our hydrologic model, they represent approximately 80% of all pollution. Agriculture is the chief contributor. This statistic is not new nor controversial, as non-point sources of pollution, and agriculture in particular, are widely known as the leading sources of nutrient pollution today. However, our analysis highlights the importance of considering the economic value of this pollution. We find that non-point sources contribute 47% of GED. Agriculture's contribution to damages (36%), while significant, is substantially less than its contribution to overall pollution levels (67%). Point sources, primarily wastewater treatment facilities, represent approximately 22% of pollution loads, but account for over half of GED (53%) due to their close proximity to people.

This study contributes to several strands of literature. First, we contribute to a growing literature related to environmental statistics and natural capital accounting. Our work most closely resembles research efforts that have used IAMs to measure the GED of climate and local air pollution (Muller and Mendelsohn, 2007, 2009; Muller et al., 2011; Tschofen et al., 2019). Cropper and Park (2023) describe these advances, while noting that the development of similar metrics for water pollution damages has lagged behind that of air pollution. We believe our study provides the first national measures of GED for water pollution for any country. Other related work has focused on measuring the value of natural capital and ecosystem services for inclusion in national accounting frameworks (Fenichel and Abbott, 2014; Fenichel et al., 2016; Ouyang et al., 2020; Fenichel, 2024), which nests into a much larger literature that has sought to develop more inclusive measures of wealth to supplement national income statistics more broadly (Arrow et al., 2012; Polasky et al., 2015; The World Bank, 2024). The foundation for this work has a long history. Muller et al. (2025) provide an excellent overview and note that Irving Fisher wrote over 100 years ago about the importance of a more comprehensive definition of wealth, citing examples of the value of fisheries, public parks, and freedom. From their first widespread use in the early 20th century, many have noted the limitations of national income statistics as a measure of well-being (Abraham and

Mackie, 2006; Rockoff, 2020).

Second, we contribute to decades of research that seeks to measure the economic damages of surface water pollution. Most revealed preference studies focus on water-based recreation and housing market impacts and most studies are local or regional in scale (Bockstael et al., 1987; Leggett and Bockstael, 2000; Phaneuf et al., 2000, 2008; Egan et al., 2009; Olmstead, 2010; Walsh et al., 2011; Keiser and Shapiro, 2019; Guignet et al., 2022; Kuwayama et al., 2022). A small, but growing number of papers examine benefits of water quality improvements using national-scale data (Keiser, 2019; Mamun et al., 2023). An alternative stated preference literature has provided complementary estimates of the value of water quality (Desvousges et al., 1987; Van Houtven et al., 2007; Bateman et al., 2023). These estimates have served as the foundation of USEPA-led IAMs to measure the benefits of national-scale policies and regulatory analyses (Carson and Mitchell, 1993; Bingham et al., 2000; Griffiths et al., 2012; USEPA, 2015). Related work has sought to measure the national damages from soil erosion and nutrient pollution, and several studies have been motivated by the US Department of Agriculture's need to measure the benefits of national conservation programs (Clark, 1985; Ribaudo, 1986; Hansen and Ribaudo, 2008; Dodds et al., 2009). To date, no work has provided national-scale, spatially-explicit estimates of marginal damages or GED for use in a national accounting framework. In addition to providing these estimates, our approach is also distinct in that we develop the micro-foundations from which one can utilize estimates from individual revealed preference studies to measure the economic damages of water pollution across many uses and at a national-scale.

A third related literature highlights the importance of economic geography and the spatial nature of pollution. The textbook description of efficient pollution policies requires setting marginal damages equal to marginal abatement costs (Baumol and Oates, 1988; Phaneuf and Requate, 2016). Implementing this basic concept at a granular level across a large area of space (i.e., a country) has been challenging. Until recently, there have been few estimates of marginal damages of local pollutants across a large spatial extent (Muller and Mendelsohn, 2007, 2009; Keeler et al., 2016; Hsiang et al., 2019). Most prominently, local estimates of air pollution damages have paved the way for a host of impactful insights ranging from the distributional consequences of environmental policy (Fowlie and Muller, 2019) to the benefits of renewal energy (Cullen, 2013; Fell et al., 2021), electric vehicle adoption (Holland et al., 2016) and the returns on energy efficiency programs (Fowlie et al., 2018), as well as the role of economic geography more broadly (Hollingsworth et al., 2024), among others. We are unaware of nationwide, local estimates of marginal damages of water pollution. This lack of damage estimates prevents similar analyses of water-related policies, as well as the ability

to explore multi-media impacts (Keiser and Muller, 2017). This paper fills this gap.

The paper proceeds as follows. We present our conceptual model of economic damages in Section 2. We then highlight important components of our hydrological model (Section 3) and describe the damage functions for individual uses of water resources (Section 4). Section 5 summarizes estimates of spatially explicit marginal damages and GED by primary sources of pollution. Section 6 concludes. Our Appendix describes each of our model components in more detail.

2 Background and Conceptual Model

2.1 Conceptual Model of Damages

In our framework, damages from nutrient pollution arise locally from three types of household interactions with surface water quality. These include amenities, recreation, and drinking water services. Damages also arise globally through a climate change mechanism. The following stylized model briefly illustrates these mechanisms and provides the conceptual basis for our empirical IAM. Additional details are described in Appendix A.

The landscape is divided into a continuum of N residential locations. There are waterbodies with varying water quality levels distributed in space across the landscape. The concentration of nutrient pollutants in a waterbody j is denoted c_j. There are H households that live in the landscape. Each household takes as given the common set of residential locations, waterbodies, and water quality levels. Households maximize utility by selecting a residential location and taking recreation trips to each of the J waterbodies.

To ground our framework in the the canonical recreation demand and hedonic property value models, we add the following structure. First, a residential location n conveys three local attributes: a bundle of neighborhood characteristics ζ_n, a local waterbody indexed $j = n$ with local nutrient concentration c_n, and a water utility that sources drinking water from the local waterbody. Second, we assume that location n provides fixed travel distances to the $J-1$ nonlocal waterbodies, so that households in location n have exogenous travel cost TC_{nj} for $j \neq n$. Finally, we assume that location n provides a continuum of available distances to the local waterbody. In equilibrium, the annual rental cost for a home in location n is $P(d_{hn}, c_n, \zeta_n) + \tau_n$, where d_{hn} is the distance that household h lives from local waterbody n and τ_n is an additively separable annual fixed tariff paid to the local water utility. Households select a residential location n, which endows them with the local waterbody, travel costs TC_{nj}

for $j \neq n$, and τ_n. They also select the distance to the local waterbody and recreation visits to the local and nonlocal waterbodies.

This structure allows us to connect nutrient pollution to social costs through three mechanisms. In Appendix A we start with a quasi-linear in income utility function U that includes amenity services from the local waterbody $A(d_{hn}, c_n)$. Amenity services are decreasing in both distance to the local waterbody and nutrient pollution. The utility function also includes recreation trips to the nonlocal waterbodies $X_{hj}(c_j)$ for $j \neq n$ and trips to the local site $X_{hn}(c_n)$. Trips are decreasing in nutrient pollution. Finally, nutrient pollution can influence the cost of treating drinking water and hence the drinking water tariff so that $\tau_n'(c_n) > 0$. Under our assumptions, the marginal damage to household h living in location n (holding location fixed) from a change in water quality in the landscape is

$$MD_{hn}(c_1, ..., c_J) = \tau_n'(c_n) - \frac{\partial U}{\partial A}\frac{\partial A(d_{hn}, c_n)}{\partial c_n} - \sum_{j=1}^{J}\frac{\partial U}{\partial X_j}\frac{\partial X_{hj}(c_j)}{\partial c_j} \tag{1}$$

2.2 Total Marginal Damages and Gross External Damages

Equation (1) derives the marginal damage for a single household from a generic marginal change in nutrient concentrations across the landscape. Our main interest is in the total marginal damage from a change in nutrient loadings (emissions) at specific points in space.[4] To derive this, we express nutrient concentrations as a stylized function of emissions $E_1, ..., E_J$ into the waterbodies so that $c_j = c_j(E_1, ..., E_J)$. Based on this, the change in concentration $\triangle c_j$ at waterbody j from a change in loadings $\triangle E_k$ into waterbody k is determined by the hydrological relationship

$$\triangle c_j = \frac{\partial c_j(E_1, ..., E_J)}{\partial E_k}\triangle E_k, \quad \forall j \tag{2}$$

Combining (1) and (2), the total marginal damage (TMD) from a change in loadings $\triangle E_k$ into waterbody k is

$$\begin{aligned} TMD(\triangle E_k) = &\sum_{n=1}^{N} H_n \tau_n'(c_n)\triangle c_n - \sum_{n=1}^{N}\sum_{h=1}^{H}\frac{\partial U}{\partial A}\frac{\partial A(d_{hn}, c_n)}{\partial c_n}\triangle c_n \\ &- \sum_{h=1}^{H}\sum_{j=1}^{J}\frac{\partial U}{\partial X_j}\frac{\partial X_{hj}(c_j)}{\partial c_j}\triangle c_j + \sum_{j=1}^{J} GHG_j(\triangle c_j), \end{aligned} \tag{3}$$

[4]This follows from a similar approach outlined by Muller and Mendelsohn (2007, 2009) for air pollution.

where H_n is the number of households living in location n and GHG_j denotes damages from greenhouse gas emissions arising from the change in nutrient concentration at waterbody j. We refer to the first term as the drinking water mechanism, the second as the amenity mechanism, the third as the recreation mechanism, and the last term as the climate change mechanism. In later sections we discuss how these are empirically measured.

To estimate the Gross External Damages (GED) attributable to a sector s from its nutrient loadings into the J waterbodies we use

$$GED_s = \sum_{k=1}^{J} TMD(\triangle E_k) \cdot E_{sk}, \tag{4}$$

where E_{sk} is the baseline emissions from sector s into waterbody k.

3 Hydrology and Pollution

We rely on the National Hydrography Database (NHD) Plus V2 and the U.S. Geological Survey's (USGS) SPARROW model for four key components. First, the NHDPlusV2 provides the base map for water resources in HydroEcon and details how water moves throughout the hydrologic network. In total, HydroEcon uses 2.7 million river segments that are, on average, less than 2km in length, over 350,000 lakes that have surface area greater than 0.01km^2, and over 2,100 watersheds (see Appendix B). Second, we link the NHDPlusV2 to the USGS SPARROW model so that we can observe baseline local concentration estimates of Total Nitrogen (TN) and Total Phosphorus (TP), our two key measures of nutrient pollution. Third, we use decay rates from the SPARROW model and river routing from the NHDPlusV2 to predict how local and downstream concentrations change as we add marginal loads of nutrients to a particular river segment. Fourth, the USGS SPARROW model provides estimates of the total pollution loading (e.g., quantity of emissions) by major sources in each watershed.

The USGS SPARROW is often described as a hybrid hydrological model that marries a biophysical model of water pollution routing and decay with a non-linear statistical model that estimates the contributions of pollution from various sources. It provides predictions of long-run average pollution concentrations and contributions. Many of the behavioral responses that we model in the next section are a function of long-run conditions, making the SPARROW model's predictions suitable for our setting.

We combine results from five regional SPARROW models that provide predictions of nutrient concentrations and loads for the conterminous US. These models include the Northeast, Southeast, Midwest, Southwest, and Pacific. Each of these regional models provides estimates of average conditions over the period 1999 to 2014 and reflect estimates of loads around 2012. While each model has the same foundational structure, there are some differences across models in terms of the predicted contributing sources and the underlying data used to calibrate each model. For instance, each regional model estimates nutrient contributions for the primary categories of municipal wastewater facilities, fertilizer runoff, and urban runoff. However, each model also includes some modest differences in other sources. For example, the Northeast estimates phosphorus contributions from mineral erosion, while each of the other four models describe a similar category of contributions from "natural sources." Appendix B describes these regional SPARROW models in more detail.

Appendix Figure B.1 displays baseline pollution concentrations and loads for nutrients across the continental U.S. As expected, nutrient concentrations are highest in the Midwest due to agriculture's outsized role in contributing to nutrient pollution. Coastal areas also have high concentrations due to large urban centers and nutrient pollution from municipal waste. There are no clear breaks in predicted concentrations or loads across the five regional models, giving greater confidence in our use of these models to represent the nation as a whole.[5]

An important contribution of this paper is the development of new routines that allow us to quickly assess how marginal changes in nutrient pollution move within and across watersheds and the resulting economic damages associated with these changes. To measure damages, we simulate adding a marginal load of nutrients in each individual river segment, trace how those nutrients travel downstream, and identify how concentrations change in each affected watershed. We then repeat this procedure for the majority of our 2.7 million river and lake segments to estimate segment-specific marginal damages.[6] This procedure is an

[5]The five individual models are the result of a coordinated effort to represent the continental US using common methodology, underlying data sources, and computational techniques. Assembly and preprocessing of water quality and stream flow data used in the five regional models was completed in a single step as reported in Saad et al. (2019). The inputs and outputs from the models are fully comparable, while allowing regional heterogeneity to be reflected in the model-specific parameterizations. See Appendix B for more details.

[6]We restrict this algorithm to the 2.5 million river segments that fall completely within a corresponding HUC8 to simplify reporting average marginal damages at the watershed level. This restriction does not impact total GED because GED is calculated using watershed-specific loads combined with the average MD of each watershed. We use all 2.7M river and lake segments for routing purposes and to determine how local and downstream concentrations change as a result of pulses in these 2.5M segments.

operationalized version of equation 2 that relates a marginal change in nutrient load at a point in space to changes in local and downstream nutrient concentrations. Our algorithm for each segment i specific pulse is as follows:

i. We first calculate an unweighted watershed average of annual TN and TP loads.

ii. Next, we calculate "marginal" loads of TN and TP that are equal to 1% of the nationwide average watershed values.[7] These represent ΔE_k in equation 2. In sensitivity analyses, we examine how damages change when we consider marginal loads that represent 5% and 10% of average watershed nutrient loads.

iii. For each river or lake segment i, we add ΔE_k to the long-term average flux for that segment. We refer to this as an emission pulse. We do this pulse one river segment at a time.

iv. For each segment i, we then compute the change in long-term average nutrient flux (nutrients passing through the segment) for all river and lake segments that are downstream from segment i following the pulse.[8] We compute the resulting change in long-term average concentration from the change in flux at all downstream segments using the long-term average flow for the segment. The pulse decays as it moves downstream according to decay rates given by SPARROW.

v. To measure marginal damages that result from these changes in concentrations, we calculate the change in all watershed concentrations as a flow-weighted average of concentration changes at all river or lake segments contained in watersheds that are impacted by this pulse. This generates Δc_j in equation 2 for the reference watershed $(j = k)$ and all downstream watersheds.

4 Damage Modules

Here, we describe the four damage modules for HydroEcon. These modules link changes in water quality conditions to changes in economic value. They include four of the most likely category of damages due to nutrient pollution, including impacts on recreation, housing, drinking water treatment, and climate change.

[7] These values are 1,959 kg/yr for TN and 15,867 kg/yr for TP.

[8] We use loads to refer to nutrient emissions at a point in space and flux to refer to the physical amount of pollution passing through a river or lake segment. Long term average flux depends on upstream and local loads.

4.1 Recreation

The impact of water quality on water-based recreational uses has been a fundamental area of research in environmental economics for decades. We estimate the lost recreation value from a change in water quality using three main steps.

First, we define a representative individual, the set of available destinations, and baseline water quality. The representative individual is defined at the census tract (ct) level. The set of available destinations for the individual – referred to as the choice set – includes lakes that are larger than 0.1km^2 and within 100 miles of the center of the census tract. We use J_{ct} to denote the lakes in the choice set. For baseline water quality, we calculate a weighted average that reflects the size of the lakes within the choice set, their distance to the representative individual, and nutrient concentrations. Specifically, for nutrient concentration c_j at each of the $j = 1, \ldots, J_{ct}$ lakes, we assign water quality for the census tract according to

$$WQ_{ct} = \sum_{j=1}^{J_{ct}} \frac{\frac{a_j \cdot c_j}{d_{ct,j}}}{\sum_{j=1}^{J_{ct}} \frac{a_j}{d_{ct,j}}}, \tag{5}$$

where a_j is the area of the lake j and $d_{ct,j}$ is the distance from the census tract center to the lake. We use total phosphorus concentration to measure c_j in the recreation module.

Next, we link total phosphorus concentrations to the number of water-based recreational days that the representative individual takes in a year. For this, we rely on a study from Keiser (2019) that finds strong evidence of a causal link between phosphorus pollution and water-based recreational use in the U.S. His research design exploits upstream sources of pollution as an instrument for local phosphorus concentrations. Keiser (2019) models recreation behavior based on lake water quality, which drives our decision to focus on lakes for our recreation module. His data records recreation visits that are for swimming in natural bodies of water, cold and warm-water fishing, boating (with a motor), and visits to noncoastal waterbodies for other recreational purposes.

We follow the functional form in Keiser (2019) and assume that a representative person in census tract ct makes annual visits to lakes based on

$$X_{ct} = \exp\left(\beta_0 + \beta_1 Z_{ct} + \beta_{wq} WQ_{ct}\right), \tag{6}$$

The number of trips per year depends on census tract variables Z_{ct} that include both location and socioeconomic characteristics as well as water quality. Parameter values are

drawn from Keiser (2019), which we use to predict the change in trips from a change in water quality according to

$$\Delta X_{ct} = exp(\beta_0 + \beta_1 D_{ct}) \cdot [exp(\beta_{wq}(WQ^1_{ct}) - exp(\beta_{wq} WQ^0_{ct})],$$

where superscripts 0 and 1 denote baseline and changed water quality levels, respectively.

We then ascribe a value to each water-based recreational day that is lost following a decrease in water quality. Specifically, if we assume a constant recreation day value (RDV) of a trip, the total lost recreation value associated with the water quality change can be estimated using

$$\Delta RV_{ct} = \Delta X_{ct} \cdot RDV \tag{7}$$

We set RDV at $70 per day in 2016 dollars based on the Oregon Recreation Use Value Database (2016) for water-based recreational use. We multiply the representative agent recreation costs from equation (7) by the adult population in the census tract to recover the total change in recreation value for the census tract. Appendix C.1 provides additional details.

4.2 Hedonics

Hedonic property value models have long been utilized to quantify the amenity value stemming from water quality changes at the local level (e.g., within a single lake, watershed, county, or state; for a review, see Guignet et al. (2022)). More recently, Mamun et al. (2023) conducted a national-scale hedonic property value analysis using sales that occurred in proximity to over 1,600 freshwater lakes across the country. They found that a 1% increase in water clarity, measured by Secchi Disc depth, on average leads to 0.18% and 0.04% increases in the value of single-family homes within 100 meters and between 100 and 300 meters from the lakeshore, respectively. Our analysis relies on the findings from this study to link changes in water quality to home values.

We begin by merging the waterbody shapefile of NHDPlusV2 with information from the Core Logic assessment database to calculate the number of properties and total assessed value of single family houses within 100 meters and between 100 and 300 meters from the shore for all lakes greater than 0.1km^2. We identify a total of 3.51 million single family residential houses located within 300 meters of 31,597 different lakes. Next, we assign each lake in a HUC8 the average watershed value for total phosphorus concentration from our SPARROW

model. To link changes in total phosphorus to a change in water clarity, we empirically estimate the relationship between Secchi depth and total phosphorus while accounting for ecosystem heterogeneity by including ecoregion fixed effects and other environmental factors in the regression. We believe this is a reasonable linkage given that nutrients are a major factor in determining water clarity (Keeler et al., 2012, 2016).

We calculate the annualized marginal damage from a change in nutrient concentration at lake j according to

$$\Delta HV_j = \alpha \cdot \left(V_j^1 \cdot \eta_1 + V_j^2 \cdot \eta_2\right) \cdot \left(\frac{\nu_j \cdot \%\Delta c_j}{100}\right). \tag{8}$$

In this expression, $\eta_1 = 0.18$ and $\eta_2 = 0.04$ are the elasticities of home price with respect to water clarity for properties in the $<$ 100m and 100-300m distance from shoreline bands, respectively, and V_j^1 and V_j^2 denote the aggregate value of the housing stock near lake j in the two distance bands. In the second term, ν_j is the elasticity of water clarity with respect to total phosphorus. The elasticity for lake j takes one of nine values ranging from 0.39 to 0.50, based on the ecological region where the lake is located. The term $\%\Delta c_j$ is the percent change in phosphorus concentration in lake j. Their product is the percentage change in water clarity generated by the increase in total phosphorus concentration in lake j. Finally, α=0.0448 is an annualization rate that translates changes in the value of the housing stock into a yearly flow value. We rely on Bishop et al. (2025) for this value. Appendix C.2 provides additional details of our hedonic approach.

4.3 Drinking Water

Nutrient water pollution generates external costs for drinking water facilities that draw raw water from surface water and groundwater and process it to supply potable water to consumers. To protect public health, the USEPA sets a limit of 10 mg/L for nitrate in finished drinking water. When nitrate levels in raw water exceed this threshold, community water systems (CWSs) must treat the water using methods such as altering intake sources, blending water, sourcing low-nitrate raw water, or applying nitrate removal technologies like reverse osmosis and ion exchange. However, the treatment involves additional costs in the form of capital, labor, energy and chemicals for the treatment process, which are ultimately passed through to the households. In this section we describe how we construct an empirical representation of these costs, which corresponds to the first term in equation (3).

We sketch our basic steps here and provide additional details in the Appendix. First, drawing on the EPA's Safe Drinking Water Information Systems (SDWIS) data, we identify

the set of CWSs that source raw water from surface waterbodies.[9] Among the over 49,000 CWSs in the US, approximately 11,000 systems source from surface water. These water systems are of different sizes based on the population they serve, and they have intakes spread across 1,070 HUC8 watersheds. We assign water quality for each CWS based on our SPARROW model prediction for total nitrogen concentration in its home HUC8 watershed.

Not all CWSs treat for nitrate and the SDWIS does not report which systems do. To determine the systems that incur abatement costs, we use assumptions based on historic nitrate levels, nitrate violation history in the recent past (2018-2022), and ownership of nitrate removal technologies. With these, we arrive at a set of 795 community water systems that we assume incur treatment costs. These systems are the basis for our calculations.

We rely on data and results from Mosheim and Ribaudo (2017) to estimate the drinking water treatment cost of an increase in nitrogen concentration. The authors report variable cost elasticities with respect to nitrogen removal of ϵ_l=0.003 and ϵ_s=0.04 for large and small systems, respectively. The data includes values for the variable costs of CWS operations among systems in the sample. We use sample variation in variable costs (VC) across geography and large versus small systems to assign VC_n^f for each plant n that treats its raw water, where $f = l, s$ indicates if the system is large or small. We assume that a percentage increase in total nitrogen concentration in a system's source water implies an equal percentage increase in abatement requirements. Based on this we calculate the change in drinking water treatment costs for a system n from a change in nutrient pollution according to

$$\Delta DW_n^f = VC_n^f \cdot \left(\frac{\epsilon_f \cdot \%\Delta c_n}{100} \right), \tag{9}$$

where $\%\Delta c_n$ is the percentage change in nitrogen concentration in the HUC8 where the system sources its water from.

4.4 Climate Change

Nutrient concentrations in surface water contribute to eutrophication in lentic ecosystems (lakes and impoundments), and this generates emissions of greenhouse gases such as methane (CH_4), carbon dioxide (CO_2), and nitrous oxide (N_2O) (DelSontro et al., 2018; Beaulieu et al., 2019). Indeed, aquatic ecosystems are the largest contributor to global methane

[9] Nitrate contamination of groundwater is an important human health issue. However, the focus of this study is on surface water pollution.

emissions (Rosentreter et al., 2021). In this section we describe how we estimate climate change damages from methane emissions that arise from increased nutrient pollution.

We use the methods described in Downing et al. (2021) to derive equations linking changes in phosphorus concentrations in lakes and reservoirs to annual changes in methane emissions and economics damages. We first use the waterbody shapefile NHDPlusV2 to identify 353,029 lakes larger than 0.01 km^2 across the US. We exclude the Great Lakes and the Great Salt Lake. An individual lake is our unit of analysis and so we link each lake to the SPARROW model output to assign a baseline water quality level for total phosphorus. The equations linking CH_4 and eutrophication are based on chlorophyll a ($chla$) concentration and so we convert total phosphorus concentration c_j in lake j to chlorophyll a concentration using McCauley et al. (1989):

$$\log_{10}(\text{chla}_j) = 0.7246777624 \cdot \log_{10}(c_j) - 0.1313111819. \tag{10}$$

To predict methane emissions from eutrophication, DelSontro et al. (2018) analyzed historical data from diverse lentic ecosystems to generate a prediction for CH4 emissions based on chlorophyll a concentrations according to

$$\log_{10}(\text{CH}_{4,j}) = 0.94 + 0.778 \log_{10}(\text{chla}_j), \tag{11}$$

where the units for CH_4 are mg per m^2 of surface area per day. We use equations (10) and (11) and the surface areas of lakes to predict how an increase in phosphorus concentration Δc_j generates additional annual methane emissions $CH_{4,j}$ from lake j.

To assign costs to the emission changes we use the social cost of one metric ton of methane in the current year, based on USEPA (2022). Using a 2% discount rate we assign $SCM = \$1799$ and calculate the annual social cost from a change in methane emissions in lake j based on

$$\Delta CC_j = \Delta CH_4(\Delta c_j) \cdot SCM.$$

5 Results

5.1 Damages by Location

Table 1 reports marginal damages and GED by U.S. Census regions. Panel A reports damages that account for pollution transport and fate. These estimates include both the watershed of origin ("local") and as well as watersheds that are impacted downstream ("downstream impacts"). Panel B reports only damages that occur within the watershed in which

the pollution is emitted. Column (1) reports average marginal damages by Census Region. We see that marginal damages are highest in the West ($1,019/kg) and Northeast ($822/kg) and considerably lower in the South ($221/kg) and Midwest ($161/kg).

Panel A of Figure 1 provides the corresponding visual representation of these results by watershed. Panel B displays corresponding GED estimates. These maps show areas where GED and marginal damages have similar patterns, as well as where they diverge. Marginal damages and GED appear higher in population centers near the coasts and near large bodies of freshwater, such as the Great Lakes and in water-rich areas such as Appalachia. Table 1, Column (2) summarizes GED by region. Here, Total GED is highest in the West and lowest in the Northeast. Although marginal damages are five times lower in the South and Midwest relative to the West, Total GED are relatively higher in these regions due to high levels of pollution loads and the fact that GED reflects both marginal damages and quantities. This is evident visually, as there are large portions of the Mississippi River Basin with low marginal damages, but high GED. On the other hand, while the Northeast has high marginal damages, it has lower levels of pollution, and thus lower overall GED. Total GED for the U.S. is approximately $140B annually.

Next, we examine the spatial concentration of total damages. In Figure 2, we rank all watersheds in the US according to their level of GED and normalize this ranking from 0 to 1. This value is captured by the x-axis. On the y-axis, we plot the corresponding cumulative share of GED. Thus, if pollution damages were evenly distributed across watersheds, we would witness a 45-degree line. Instead, we see that damages are highly concentrated in a small fraction of watersheds. The top 20 percent of watersheds as ranked by GED are responsible for over 80% of GED. We also plot the location of these watersheds. Many of these top watersheds fall near high population centers and a number of these trace out portions of the Mississippi River.

5.2 Cross-boundary Pollution

Next, we examine how the transport and fate of nutrient pollution impacts downstream communities. In Table 1, Panel B, we report the amount of marginal damages and GED that only accrue from within the watershed in which the pollution is generated. We find that the local component of marginal damages is approximately 80% on average. This figure varies from approximately 69% in the Midwest to 88% in the Northeast. Approximately 86% of damages are local in the West and 74% in the South. This suggests that a meaningful component of marginal damages arise due to their non-local impacts on water users. The

share of local contributions to GED are nearly identical to that of marginal damages at the national level (80%) and the variation across regions follows a similar pattern as marginal damages.

By comparing Panels A and B of Table 1 we are able to analyze the importance of hydrological boundaries in measuring damages. Columns (3) and (4) also highlight the spillover of pollution across political boundaries. Columns (3) and (4) of Panel A shows that approximately 80% of total GED accrue within state boundaries, meaning that a material amount of damages (20%) are born by downstream states. While the percent of national damages that are in-state are similar to the national percentage of damages that are confined to local watersheds, these percentages vary more widely across census regions. The percentage of damages that are in-state are 54% in the Northeast, 70% in the Midwest, 80% in the South, and 95% in the West.

5.3 Uses of Water Resources

In Table 2, we explore how different uses of water resources contribute to our estimates of damages. In Columns (1) and (2), we display estimates of damages that account for local and downstream impacts. In Columns (3) and (4), we examine the extent to which these damages are driven by local impacts. The most immediate finding from this table is that recreational use comprises the largest share of damages. 94% of marginal and gross external damages can be attributed to impacts on water-based recreational use. This finding is likely driven by the fact that such a large share of the U.S. population participates in some water-based recreational activity (approximately two-thirds) and a large share of the population lives near water bodies that may be impacted by nutrients. This finding is also consistent with the general notion that the largest share of water quality benefits likely accrue to water-based recreational users (Freeman, 1982; Olmstead, 2010; Keiser et al., 2019).

Climate change and housing impacts are also important components of damages, though contribute significantly less to marginal damages and GED. Their share of GED are approximately 3% and 2%, respectively. While relatively small compared to recreation, overall damages are still substantial at $5B and $3B annually. Drinking water treatment impacts provide the smallest contribution to damages. One important caveat is that drinking water damages represent treatment costs and exclude any potentially important human health impacts that may arise from any residual or untreated pollution.

Figures 3 and 4 display the corresponding variation in marginal and gross external damages by watershed by use. Both marginal and gross external damages for recreation largely

follow the same patterns as seen in Figure 1. This is unsurprising given the significant contribution of this category to overall damages. Other use categories display interesting patterns. Housing impacts show significant clusters of watersheds where marginal damages are particularly high, while marginal damages are more evenly spread out for climate change and drinking water treatment. In terms of GED, overall damages for most use categories are higher on the coasts and in the eastern half of the United States. GED from drinking water treatment impacts are generally larger in the Midwest and the northern half of the country.

5.4 Industry Contributions

Table 3 reports marginal and GED by source, as well as total emissions by source. Here, we report emissions for phosphorus, as it is responsible for over 99% of damages. As is well-documented, agriculture is responsible for the largest share of emissions (Column 1). It is responsible for 66% of anthropogenic sources of nutrient pollution (200 thousand metric tons per year). Municipal wastewater contributes 22% of overall pollution loads (65 thousand metric tons) and urban run-off is estimated to contribute 12% (37 thousand metric tons). However, one of the most striking findings from this analysis is that while agriculture is responsible for a majority of pollution, municipal wastewater contributes the largest share of GED. It is responsible for over half of all damages ($57B/yr). While still significant, agriculture only contributes approximately 36% of GED ($38B/yr), and urban non-point source pollution contributes 11% ($12B/yr). Column (2) suggests that this difference in pollution loads versus pollution damages is likely due to the spatial location of polluting activities. As shown in Figure 1, marginal damages are significantly lower in the Midwest, where agriculture is primarily located. Municipal point sources on the other hand are often located closer to population centers and thus contribute larger damages on the margin. These differences in marginal damages appear large enough to influence the overall contribution of these sources to GED. Figure 5 displays maps of GED by source by watershed.

6 Conclusions

This paper provides estimates of the marginal and corresponding gross external damages of nutrient pollution in US waterways. We find that marginal and gross external damages are highest near population centers and waterbodies. Damages are highly concentrated and provide strong evidence that spatially-targeted interventions may have high returns. This

pattern of spatially varying marginal damages follows similar patterns found in local air pollutants (Muller and Mendelsohn, 2009). We also find that significant shares of pollution damages are borne by individuals that live within hydrologic and political boundaries that are distinct from the sources of pollution. This finding provides support for a robust federal role in managing these pollutants.

We estimate that total GED from nutrient pollution is approximately $134B per year. In 2012, the baseline year for our pollution loading estimates, our estimates of GED were approximately 0.8% of GDP. For agriculture in particular, $38B in GED represents approximately 19% of total US farm income. The closest comparison to our estimates is work done to measure GED of air pollution in the US. Tschofen et al. (2019) estimates that total air pollution GED is approximately $790B to $1,010B per year over a similar time frame. The authors estimate that agriculture contributes approximately $230B in air pollution GED, which is approximately 6 times our estimate of nutrient pollution damages from this sector. While not as directly comparable, Dodds et al. (2009) estimates that nutrient pollution as a whole contributes around $2.2B per year in societal costs, which is significantly less than our estimate of GED.

Nearly all current discussion of US water pollution focuses heavily on the role of US agriculture. This focus is well-founded, as agriculture is responsible for the largest share of US water pollution. While we find that agriculture still contributes significantly to GED, municipal wastewater is responsible for the largest share of damages. This fact provides some preliminary support for the continued focus on abatement efforts at these treatment plants. The Clean Water Act allows regulation of point sources, but largely thwarts efforts to address non-point source pollution. Thus, wastewater treatment plants have largely been the focus of tightening pollution standards to address nutrient pollution. On the margin, controlling pollution from these sources is expensive. Our results highlight that benefits, depending on location, may also be large.

We see several important directions for future work. First, optimal pollution policy requires setting marginal damages equal to marginal abatement costs. One natural extension would be to consider these abatement options across space to find spatially-optimal levels of nutrient pollution. This information could inform a host of policy interventions, ranging from Clean Water Act programs that target wastewater treatment plants to USDA conservation programs, such as the Conservation Reserve Program and the Environmental Quality Incentives Program. The US spends billions of dollars each year on abatement efforts. Knowledge of the corresponding benefits could inform optimal policy design.

Another fruitful area of research may be to consider how damages from particular sources may vary for water versus air pollution. By combining this information on damages, policy makers and other stakeholders will have a more comprehensive picture of the benefits of controlling particular sources of pollution. In addition, our damage estimates reflect recreation, housing, drinking water treatment, and climate change impacts. Other unmeasured channels of benefits, such as health impacts, could play an important role as future studies advance our understanding of how nutrient pollution impacts ecological and human health.

Finally, though nutrient pollution is a leading cause of impairments in US waterways, there are tens of thousands of US chemicals emitted into the environment each year. A natural next step would be to model and measure the economic damages of other key pollutants, such as bacteria and biochemical oxygen demand, among others.

References

Abraham, K. G. and C. Mackie (2006). A framework for nonmarket accounting. *A New Architecture for the U.S. National Accounts*.

Arrow, K. J., P. Dasgupta, L. H. Goulder, K. J. Mumford, and K. Oleson (2012). Sustainability and the measurement of wealth. *Environment and Development Economics 17(3)*, 317–353.

Ator, S. W. (2019). Spatially referenced models of streamflow and nitrogen, phosphorus, and suspended sediment loads in streams of the northeastern united states. U.S. Geological Survey Scientific Investigations Report No. 2019-5118.

Bagstad, K. J., J. C. Ingram, C. D. Shapiro, A. L. Notte, J. Maes, S. Vallecillo, C. F. Casey, P. D. Glynn, M. P. Heris, J. A. Johnson, C. Lauer, J. Matuszak, K. L. Olseon, S. M. Posner, C. Rhodes, and B. Voigt (2021). Lessons learned from development of natural capital accounts in the united states and european union. *Ecosystem Services 52*, 101359.

Bateman, I. J., B. Keeler, S. M. Olmstead, and J. Whitehead (2023). Perspectives on Valuing Water Quality Improvements Using Stated Preference Methods. *Proceedings of the National Academy of Sciences 120(18)*, e2217456120.

Baumol, W. J. and W. E. Oates (1988). *The Theory of Environmental Policy*. Cambridge University Press.

Beaulieu, J. J., T. DelSontro, and J. A. Downing (2019). Eutrophication will increase methane emissions from lakes and impoundments during the 21st century. *Nature communications 10*(1), 1375.

Bingham, T. H., T. R. Bondelid, B. M. Depro, R. C. Figueroa, A. B. Hauber, S. J. Unger, and G. L. Van Houtven (2000). A benefits assessment of water pollution control programs since 1972: Part 1, the benefits of point source controls for conventional pollutants in rivers and streams: Final report. Technical report, Prepared by Research Triangle Institute for the Office of Water and Office of Policy, Economics, and Innovation, U.S. Environmental Protection Agency, Washington DC.

Bishop, K. C., J. Dowling, N. V. Kuminoff, and A. Murphy (2025). Tax policy and the heterogeneous costs of homeownership. *Accepted at Journal of Urban Economics*.

Bockstael, N. E., M. W. Hanemann, and C. L. Kling (1987). Estimating the value of water quality improvements in a recreation demand framework. *Water Resources Research*.

Carson, R. T. and R. C. Mitchell (1993). The value of clean water: The public's willingness to pay for boatable, fishable, and swimmable quality water. *Water Resources Research 29(7)*, 2445–2454.

Clark, E. H. (1985). The off-site costs of soil erosion. *Journal of Soil and Water Conservation 40*(1), 19–22.

College of Forestry, Oregon State University (1981-2010). Recreational use values database. Available online at http://recvaluation.forestry.oregonstate.edu/ (accessed September 10, 2013).

Cropper, M. L. and Y. Park (2023). Incorporating air and water pollution into the national income and products accounts. *NBER Working Paper Series*.

Cullen, J. (2013). Measuring the environmental benefits of wind-generated electricity. *American Economic Journal: Economic Policy 5(4)*, 107–133.

DelSontro, T., J. J. Beaulieu, and J. A. Downing (2018). Greenhouse gas emissions from lakes and impoundments: Upscaling in the face of global change. *Limnology and Oceanography Letters 3*(3), 64–75.

Desvousges, W. H., V. K. Smith, and A. Fisher (1987). Option price estimates for water quality improvements: A contingent valuation study for the monongahela river. *Journal of Environmental Economics and Management 14(3)*, 248–267.

Dodds, W. K., W. W. Bouska, J. L. Eitzmann, T. J. Pilger, K. L. Pitts, A. J. Riley, J. T. Schloesser, and D. J. Thornbrugh (2009). Eutrophication of u.s. freshwaters: Analysis of potential economic damages. *Environmental Science and Technology 43(1)*, 12–19.

Downing, J. A., S. Polasky, S. M. Olmstead, and S. C. Newbold (2021). Protecting local water quality has global benefits. *Nature Communications 12*(1), 2709.

Egan, K. J., J. A. Herriges, C. L. Kling, and J. A. Downing (2009). Valuing water quality as a function of water quality measures. *American Journal of Agricultural Economics 91(1)*, 106–123.

Fell, H., D. T. Kaffine, and K. Novan (2021). Emissions, transmission, and the environmental value of renewable energy. *American Economic Journal: Economic Policy 13(2)*, 241–272.

Fenichel, E., J. Abbott, J. Bayham, W. Boone, E. Haacker, and L. Pfieffer (2016). Measuring the value of groundwater and other forms of natural capital. *Proceedings of the National Academy of Sciences 113(9)*, 2382–2387.

Fenichel, E. P. (2024). A new era of economic measurement for the environment and natural capital. *Review of Environmental Economics and Policy 18(2)*, 321–330.

Fenichel, E. P. and J. K. Abbott (2014). Natural capital: From metaphor to measurement. *Journal of the Association of Environmental and Resource Economists 1*, 1–27.

Fowlie, M., M. Greenstone, and C. Wolfram (2018). Do energy efficiency investments deliver? evidence from the weatherization assistance program. *The Quarterly Journal of Economics 133(3)*, 1597–1644.

Fowlie, M. and N. Muller (2019). Market-based emissions regulation when damages vary across sources: What are the gains from differentiation? *Journal of the Association of Environmental and Resource Economists 6(3)*, 593–632.

Freeman, M. A. (1982). *Air and Water Pollution Control*. John Wiley & Sons.

Griffiths, C., H. Klemick, M. Massey, C. Moore, S. Newbold, D. Simpson, P. Walsh, and W. Wheeler (2012). U.s. environmental protection agency valuation of surface water quality improvements. *Review of Environmental Economics and Policy 6(1)*, 130–146.

Guignet, D., M. T. Heberling, M. Papenfus, and O. Griot (2022). Property values, water quality, and benefit transfer: A nationwide meta-analysis. *Land Economics 98(2)*, 198–218.

Hansen, L. and M. Ribaudo (2008). Economic measures of soil conservation benefits: Regional values for policy assessment. Technical report, USDA.

Holland, S. P., E. T. Mansur, N. Z. Muller, and A. J. Yates (2016). Are there environmental benefits from driving electric vehicles? the importance of local factors. *American Economic Review 106(12)*, 3700–3729.

Hollingsworth, A., T. Jaworski, C. Kitchens, and I. Rudik (2024). Economic geography and air pollution regulation in the united states. Cornell Working Paper.

Hoos, A. B. and V. L. Roland II (2019). Spatially referenced models of streamflow and nitrogen, phosphorus, and suspended sediment loads in streams of the southeastern united states. U.S. Geological Survey Scientific Investigations Report No. 2019-5135.

Hsiang, S., P. Oliva, and R. Walker (2019). The distribution of environmental damages. *Review of Environmental Economics and Policy 13(1)*, 83–103.

Keeler, B. L., J. D. Gourevitch, S. Polasky, F. Isbell, C. W. Tessum, J. D. Hill, and J. D. Marshall (2016). The social costs of nitrogen. *Science Advances 2(10)*, e1600219.

Keeler, B. L., S. Polasky, K. A. Brauman, K. A. Johnson, J. C. Finlay, A. O'Neill, K. Kovacs, and B. Dalzell (2012). Linking water quality and well-being for improved assessment and valuation of ecosystem services. *Proceedings of the National Academy of Sciences of the United States of America 109(45)*, 18619–18624.

Keiser, D. A. (2019). The missing benefits of clean water and the role of mismeasured pollution data. *Journal of the Association of Environmental and Resource Economists 6(4)*, 669–707.

Keiser, D. A., C. L. Kling, and J. S. Shapiro (2019). The Low But Uncertain Measured Benefits of US Water Quality Policy. *Proceedings of the National Academy of Sciences 116(12)*, 5262–5269.

Keiser, D. A. and N. Z. Muller (2017). Air and water: Integrated assessment models for multiple media. *Annual Review of Resource Economics 9*, 165–184.

Keiser, D. A. and J. S. Shapiro (2019). Consequences of the Clean Water Act and the Demand for Water Quality. *Quarterly Journal of Economics 134(1)*, 349–396.

Kuwayama, Y., S. Olmstead, and J. Zheng (2022). A more comprehensive estimate of the value of water quality. *Journal of Public Economics 207*, 104600.

Leggett, C. G. and N. E. Bockstael (2000). Evidence of the effects of water quality on residential land prices. *Journal of Environmental Economics and Management 39*, 121–144.

Mamun, S., A. Castillo-Castillo, K. Swedberg, J. Zhang, K. J. Boyle, D. Cardoso, C. L. Kling, C. Nolte, M. Papenfus, D. Phaneuf, and S. Polasky (2023). Valuing water quality in the united states using a national dataset on property values. *Proceedings of the National Academy of Sciences 120*(15), e2210417120.

McCauley, E., J. A. Downing, and S. Watson (1989). Sigmoid relationships between nutrients and chlorophyll among lakes. *Canadian Journal of Fisheries and Aquatic Sciences 46*(7), 1171–1175.

Mosheim, R. and M. Ribaudo (2017). Costs of Nitrogen Runoff for Rural Water Utilities: A Shadow Cost Approach. *Land Economics 93*(1), 12–39.

Muller, N. Z., E. P. Fencichel, and M. Bohman (2025). Measuring and accounting for environmental public goods: A national accounts perspective. *University of Chicago Press*.

Muller, N. Z. and R. Mendelsohn (2007). Measuring the damages of air pollution in the united states. *Journal of Environmental Economics and Management 54(1)*, 1–14.

Muller, N. Z. and R. Mendelsohn (2009). Efficient pollution regulation: Getting the prices right. *American Economic Review 99(5)*, 1714–1739.

Muller, N. Z., R. Mendelsohn, and W. Nordhaus (2011). Environmental accounting for pollution in the united states economy. *American Economic Review 101(5)*, 1649–1675.

Nordhaus, W. D. and J. Tobin (1973). *The Measurement of Economic and Social Performance*, Chapter Is Growth Obsolete?, pp. 509–564. NBER.

NRC (1999). *Nature's Numbers: Expanding the National Economic Accounts to Include the Environment*. National Academies Press.

Olmstead, S. M. (2010). The economics of water quality. *Review of Environmental Economics & Policy 4(1)*, 44–61.

Ouyang, Z., C. Song, H. Zheng, S. Polasky, Y. Xiao, I. J. Bateman, J. Liu, M. Ruckelshaus, F. Shi, Y. Xiao, W. Xu, Z. Zou, and G. C. Daily (2020). Using gross ecosystem product (gep) to value nature in decision making. *Proceedings of the National Academy of Sciences 117(25)*, 14593–14601.

Phaneuf, D. J., C. L. Kling, and J. A. Herriges (2000). Estimation and welfare calculations in a generalized corner solution model with an application to recreation demand. *The Review of Economics and Statistics 82(1)*, 83–92.

Phaneuf, D. J. and T. Requate (2016). *A Course in Environmental Economics: Theory, Policy, and Practice*. Cambridge University Press.

Phaneuf, D. J., V. K. Smith, R. B. Palmquist, and J. C. Pope (2008). Integrating property value and local recreation models to value ecosystem services in urban watersheds. *Land Economics 84(3)*, 361–381.

Polasky, S., B. Bryant, P. Hawthorne, J. Johnson, B. Keeler, and D. Pennington (2015). Inclusive wealth as a metric of sustainable development. *Inclusive Wealth as a Metric of Sustainable Development 40*, 445–466.

Preston, S. D., R. B. Alexander, M. D. Woodside, and P. A. Hamilton (2009). Sparrow modeling - enhancing understanding of the nation's water quality. U.S. Geological Survey Fact Sheet 2009 - 3019.

Ribaudo, M. O. (1986). Reducing soil erosion: Offsite benefits. Technical report, USDA.

Robertson, D. M. and D. A. Saad (2019). Spatially referenced models of streamflow and nitrogen, phosphorus, and suspended sediment loads in streams of the midwestern united states. U.S. Geological Survey Scientific Investigations Report No. 2019-5114.

Rockoff, H. (2020). Off to a good start: The nber and the measurement of national income. *NBER Working Paper Series*.

Rosentreter, J. A., A. V. Borges, B. R. Deemer, M. A. Holgerson, S. Liu, C. Song, J. Melack, P. A. Raymond, C. M. Duarte, G. H. Allen, et al. (2021). Half of global methane emissions come from highly variable aquatic ecosystem sources. *Nature Geoscience 14*(4), 225–230.

Saad, D. A., G. E. Schwarz, D. M. Argue, D. W. Anning, S. A. Ator, A. B. Hoos, S. D. Preston, D. M. Robertson, and D. Wise (2019). Estimates of long-term mean daily streamflow and annual nutrient and suspended-sediment loads considered for use in regional sparrow models of the conterminous united states, 2012 base year. U.S. Geological Survey Scientific Investigations Report No. 2019-5069.

Schwarz, G. E., A. Hoos, R. Alexander, and R. Smith (2006). The sparrow surface water-quality model: Theory, application and user documentation. U.S. Geological Survey Techniques and Methods Book 6, Section B, Chapter 3.

Smith, R. A., G. E. Schwarz, and R. B. Alexander (1997). Regional interpretation of water-quality monitoring data. *Water Resources Research 33*(12), 2781–2798.

Soranno, P. A., L. C. Bacon, M. Beauchene, K. E. Bednar, E. G. Bissell, C. K. Boudreau, M. G. Boyer, and et al. (2017). Lagos-ne: a multi-scaled geospatial and temporal database of lake ecological context and water quality for thousands of us lakes. *GigaScience 6(12)*, gix101.

The White House (2023). Fact Sheet: Biden-Harris Administration Releases National Strategy to Put Nature on the Nation's Balance Sheet. Technical report.

The World Bank (2024). The Chaning Wealth of Nations: Revisiting the Measurement of Comprehensive Wealth.

Tschofen, P., I. Azavedo, and N. Z. Muller (2019). Fine particulate matter damages and value added in the us economy. *Proceedings of the National Academy of Sciences 116(40)*, 19857–19862.

USDA (2009). National survey on recreation and the environment.

USEPA (2007). National lakes assessment. Available online at http://water.epa.gov/type/lakes/lakessurvey_index.cfm (accessed March 13, 2015).

USEPA (2015). Benefit and cost analysis for the effluent limitations guidelines and standards for the steam electric power generating point source category. Technical report, Environmental Protection Agency.

USEPA (2022). Report on the social cost of greenhouse gases: Estimates incorporating recent scientific advances.

USEPA (2024). Nutrient pollution. https://www.epa.gov/nutrientpollution , accessed January 3, 2024.

Van Houtven, G. L., J. Powers, and S. K. Pattanayak (2007). Valuing water quality improvements in the united states using meta-analysis: Is the glass half-full or half-empty for national policy analysis? *Resource and Energy Economics 29*, 206–228.

Walsh, P. J., J. W. Milon, and D. O. Scrogin (2011). The spatial extent of water quality benefits in urban housing markets. *Land Economics 87(4)*, 628–644.

Wise, D. R. (2019). Spatially referenced models of streamflow and nitrogen, phosphorus, and suspended sediment loads in streams of the pacific region of the united states. U.S. Geological Survey Scientific Investigations Report No. 2019-5112.

Wise, D. R., D. W. Anning, and O. L. Miller (2019). Spatially referenced models of streamflow and nitrogen, phosphorus, and suspended sediment transport in streams of the southwestern united states. U.S. Geological Survey Scientific Investigations Report No. 2019-5106.

Table 1: Marginal and Gross External Damages by US Census Region

	Marginal Damages ($/kg) (1)	Total GED ($B) (2)	In-State GED ($B) (3)	Downstream States GED ($B) (4)
Panel A: Local and Downstream Impacts				
Northeast	822	22.90	12.45	10.45
South	221	35.30	28.33	6.97
Midwest	161	27.97	19.85	8.13
West	1,019	53.75	51.26	2.49
U.S.	**338**	**139.92**	**111.89**	**28.04**
Panel B: Local Impacts				
Northeast	729	20.31	11.44	8.87
South	164	26.18	22.48	3.70
Midwest	111	19.26	14.66	4.60
West	880	46.41	45.62	0.79
U.S.	**271**	**112.17**	**94.21**	**17.96**

Notes: This table reports average marginal and Gross External Damages (GED) by U.S. Census Regions. Panel A displays damages that allow for downstream fate and transport of pollution. Panel B reports the portion of damages that occur within the watershed in which a pollution source resides. Columns (1) and (2) report total average marginal and GED. Columns (3) and (4) report the portion of GED that occur within the state of origin versus downstream states.

Table 2: Marginal and Gross External Damages by Use Category

	Local and Downstream Marginal Damages ($/kg) (1)	GED ($B) (2)	Local Marginal Damages ($/kg) (3)	GED ($B) (4)
Recreation	319.1	132.0	258.7	107.1
Housing	7.5	3.1	5.0	2.1
Drinking Water Treatment	0.02	0.08	0.02	0.06
Climate Change Impacts	11.4	4.7	7.3	3.0
U.S.	**338.0**	**140.0**	**270.9**	**112.2**

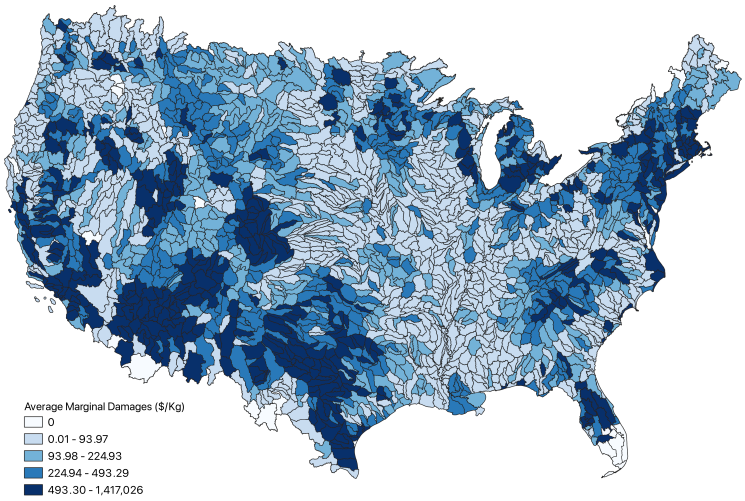
Notes: This table reports average marginal and Gross External Damages (GED) by water use. Columns (1) and (2) report total average marginal and GED. Columns (3) and (4) report the portion of marginal damages and GED that occur within the local watershed of origin.

Table 3: Marginal and Gross External Damages by Source

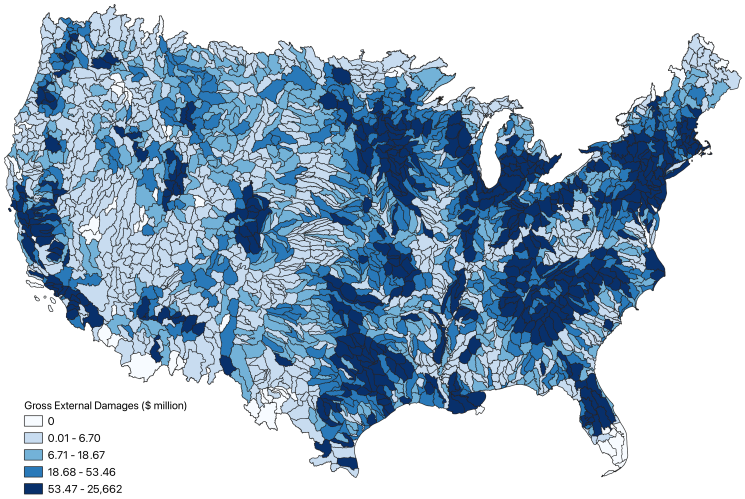
	Emissions (Metric Tons) (1)	Spatially Explicit Marginal Damages ($/kg) (2)	GED ($B) (3)
Non-Point Sources			
Agriculture	200,446	190.1	38.1
Urban	37,295	324.4	12.1
Point Sources			
Municipal Wastewater	65,336	869.4	56.8

Notes: This table reports emissions of phosphorus (Column 1), spatially-explicit marginal damages (Column 2) and Gross External Damages (Column 3) by source type. Damages vary across sources based on location, not differences in pollutant types. We report emissions of phosphorus since they are responsible for the largest share of nutrient damages in our model.

Figure 1: Average Marginal Damages and Gross External Damages by Watershed



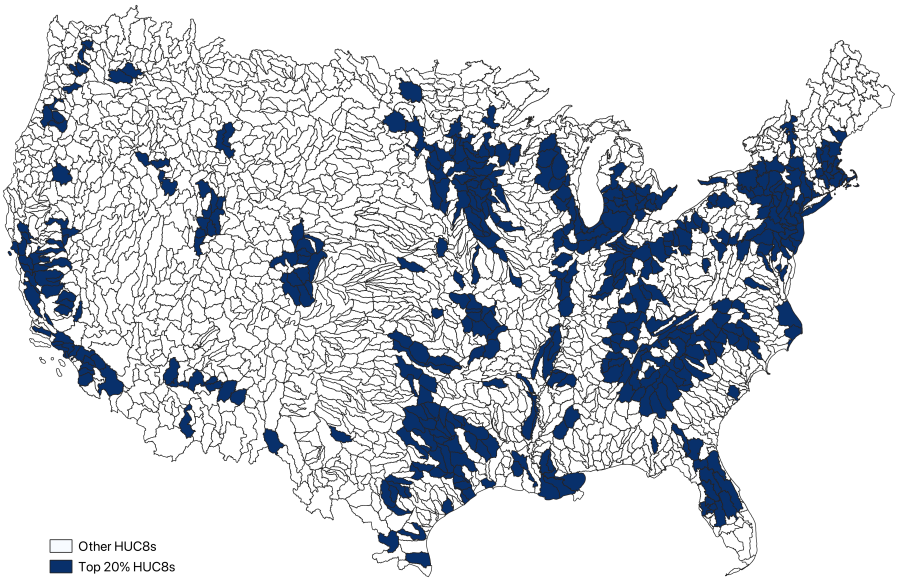
(a) Average Marginal Damages ($/kg)



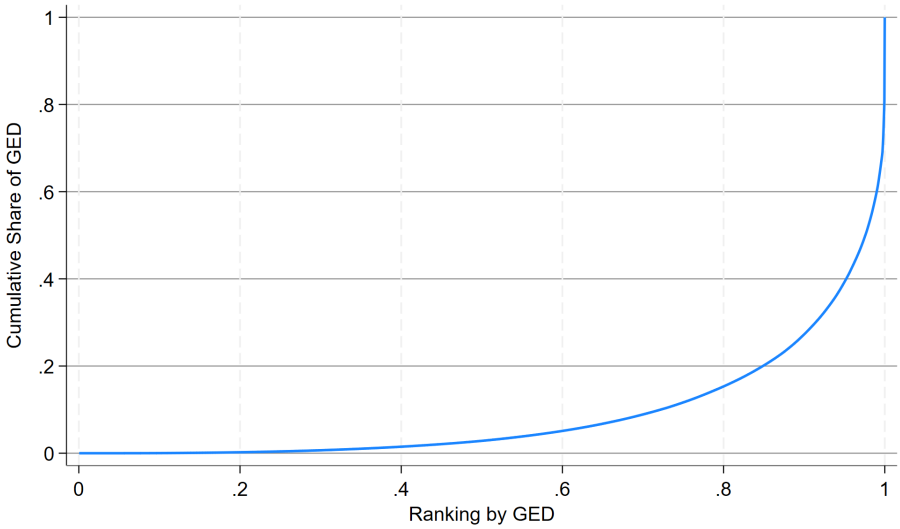
(b) Gross External Damages ($B)

Notes: Panel A displays average marginal damages by watershed. Panel B displays corresponding Gross External Damages. Darker shades of blue represent larger damages. Watersheds where damages are not estimated are displayed as white.

Figure 2: Hot Spots and Distribution of Gross External Damages



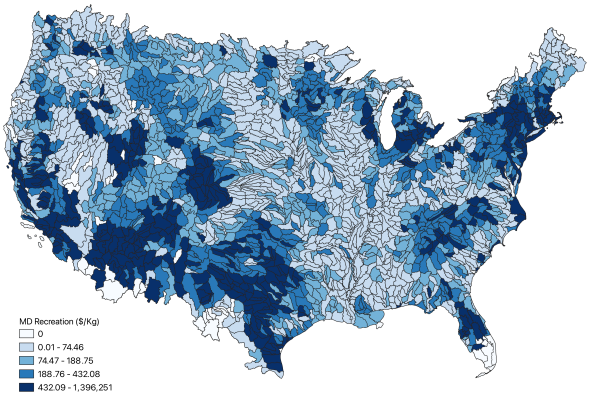
(a) GED Hot Spots



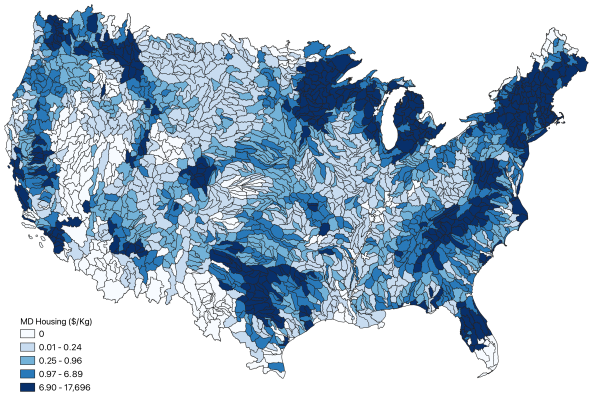
(b) Distribution of GED

Notes: Panel A displays the location of the top 20% of watersheds by GED. Panel B displays the cumulative share of GED (y-axis) by the ranking of watersheds according to GED (x-axis). Equal distribution of damages would follow a 45-degree line.

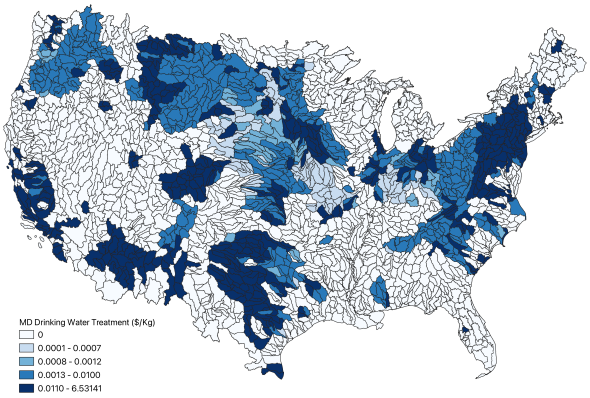
Figure 3: Average Marginal Damages by Use by Watershed



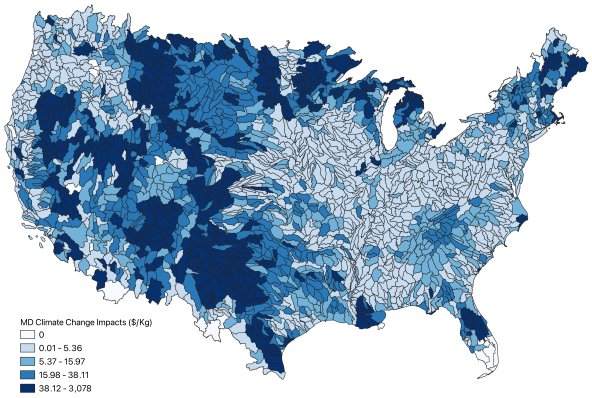
(a) Recreation



(b) Housing



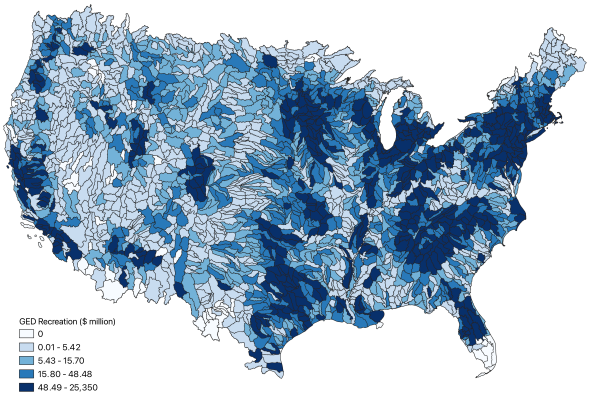
(c) Drinking Water Treatment



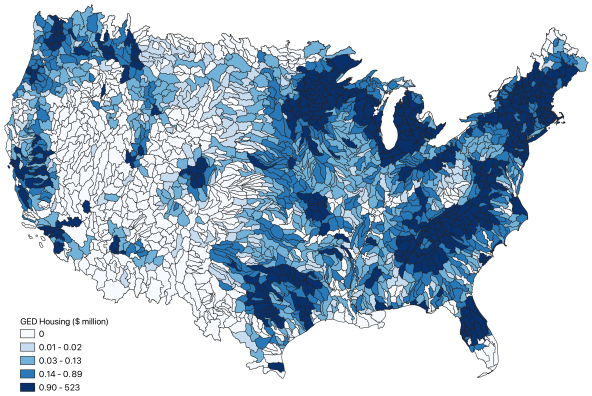
(d) Climate Change Impacts

Notes: This figure plots average marginal damages by watershed by use category. Panel a) corresponds to water-based recreation damages, Panel b) displays housing damages, Panel c) captures drinking water treatment costs and Panel d) reflects climate change impacts. Darker shades of blue represent larger damages. Watersheds where damages are not estimated are displayed as white.

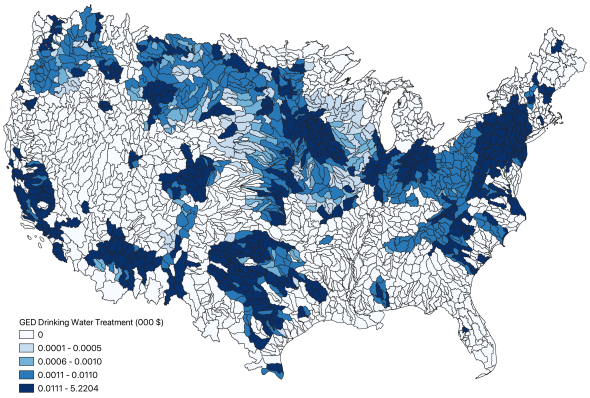
Figure 4: Gross External Damages by Use by Watershed



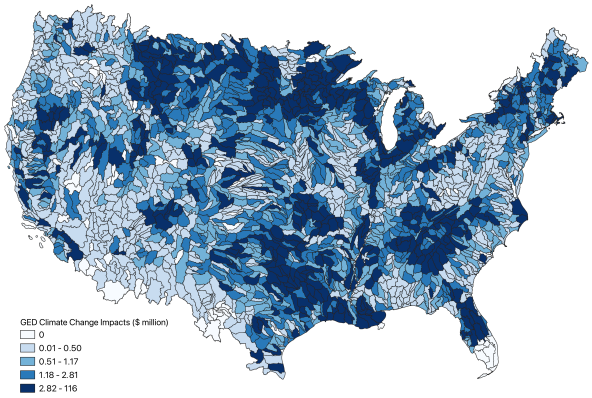
(a) Recreation



(b) Housing



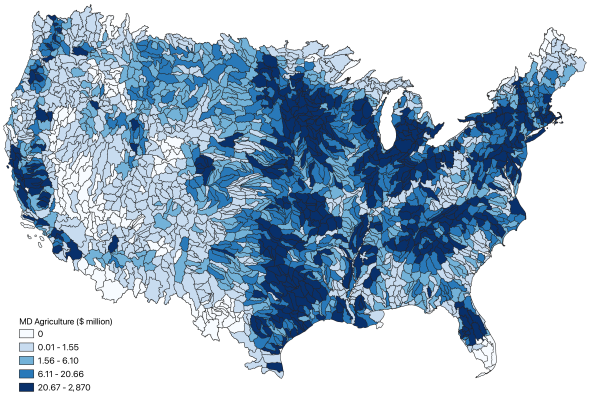
(c) Drinking Water Treatment



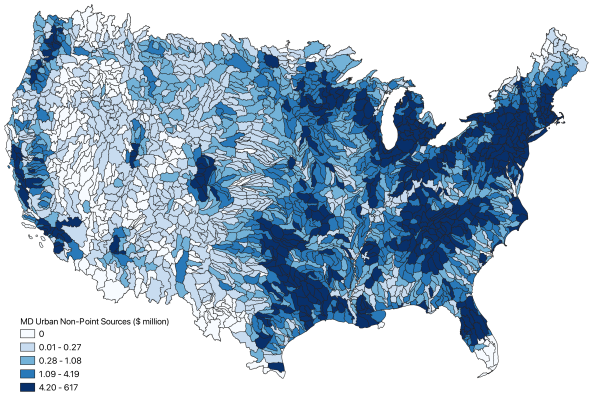
(d) Climate Change Impacts

Notes: This figure plots GED by watershed by use category. Panel a) corresponds to water-based recreation damages, Panel b) displays housing damages, Panel c) captures drinking water treatment costs and Panel d) reflects climate change impacts. Darker shades of blue represent larger damages. Watersheds where damages are not estimated are displayed as white.

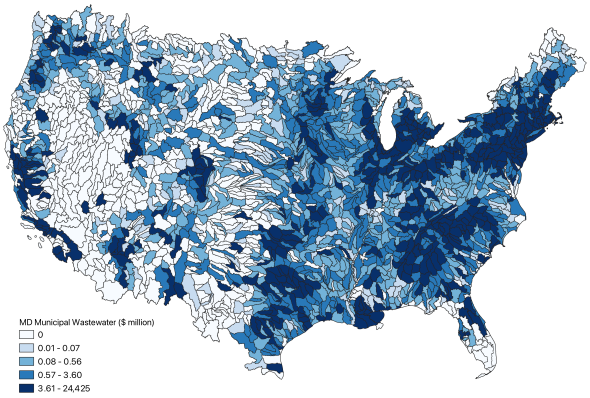
Figure 5: Gross External Damages by Use by Source



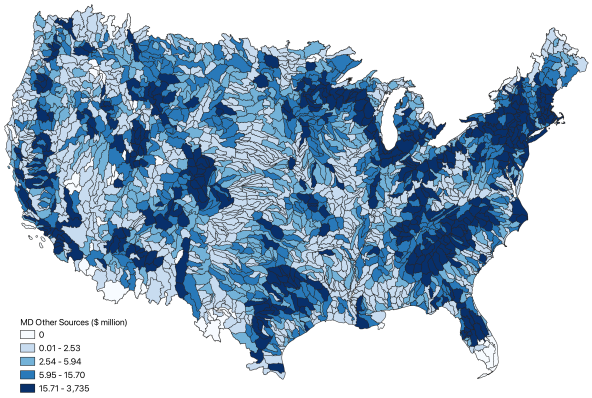
(a) Agriculture



(b) Urban Non-Point Sources



(c) Municipal Wastewater



(d) Other Sources

Notes: This figure plots GED by watershed by source. Panel a) corresponds to damages from Agricultural non-point sources, Panel b) displays damages for Urban non-point sources, Panel c) provides estimates of damages for Municipal Wastewater and Panel d) reflects other, mostly natural, sources. Darker shades of blue represent larger damages. Watersheds where damages are not estimated are displayed as white.

Online Appendix for

The Social Costs of Water Pollution in the United States

David A. Keiser Tihitina Andarge Mohammad Mainul Hoque Yongjie Ji
Catherine L. Kling Daniel J. Phaneuf Nilesh Shinde Yau-Huo Shr

March 19, 2025

A Conceptual Model

We start with a quasi-linear utility function for household h that is separable in numeraire consumption z_h and utility from local waterbody amenities, recreation trips to the J waterbodies, and local public goods:

$$U\left(A(d_{hn}, c_n), X_{h1}(c_1), \ldots, X_{hJ}(c_J), \zeta_n\right) + z_h, \tag{A1}$$

We model the residential choice set as a continuum from which households select their neighborhood by choosing values for local water quality (c_n) and local public goods (ζ_n). They determine their location within a neighborhood by choosing a distance to the local waterbody (d_{hn}). Households maximize utility by selecting these values and trips to the J recreation sites according to the budget constraint

$$Y_h = P(d_{hn}, c_n, \zeta_n) + \tau_n + tc \cdot d_{hn} \cdot X_{hn} + \sum_{j \neq n} \left(tc \cdot d_{nj} \cdot X_{hj}\right), \tag{A2}$$

where Y_h is annual income, tc is the per mile cost of traveling to a recreation site, and d_{nj} is the exogenous distance from neighborhood n to waterbody j for all $j \neq n$. Households pay an annual tariff τ_n to a local community water system (CWS) that is exogenously set to allow cost recovery for the CWS.

The first order conditions for utility maximization provide the conceptual basis for measuring the amenity and recreation costs of changes in ambient water quality. The conditions for local public goods (ζ_n) and local water quality (c_n) are

$$\frac{\partial P(\cdot)}{\partial \zeta_n} = \frac{\partial U(\cdot)}{\partial \zeta_n} \tag{A3}$$

and

$$\frac{\partial P(\cdot)}{\partial c_n} + tc \cdot d_{hn} \cdot \frac{\partial X_{hn}}{\partial c_n} = \frac{\partial U(\cdot)}{\partial A}\frac{\partial A}{\partial c_n} + \frac{\partial U(\cdot)}{\partial X_n}\frac{\partial X_{hn}}{\partial c_n}, \tag{A4}$$

respectively. Equation (A4) shows that households are willing to pay for better water quality through two channels, for two reasons. Holding d_{hn} fixed, they are willing to pay higher rent and spend marginally more on recreation trips (the left-hand side) in return for better amenity services and higher utility from recreation (the right-hand side). Furthermore, the first-order condition for X_{hn} is $\frac{\partial U(\cdot)}{\partial X_n} = tc \cdot d_{hn}$, and so (A4) can be broken out as

$$
\begin{aligned}
-\frac{\partial P(\cdot)}{\partial c_n} &= -\frac{\partial U(\cdot)}{\partial A}\frac{\partial A}{\partial c_n} \\
tc \cdot d_{hn} \cdot \frac{\partial X_{hn}}{\partial c_n} &= \frac{\partial U(\cdot)}{\partial X_n}\frac{\partial X_{hn}}{\partial c_n}.
\end{aligned} \tag{A5}
$$

This shows that in equilibrium and conditional on d_{hn}, the rent price gradient for water quality reveals the amenity mechanism marginal willingness to pay for a change in c_n, the change in recreation expenditure reveals the recreation mechanism marginal willingness to pay, and these values are additive.

The first order condition for d_{hn} is

$$
-\frac{\partial P(\cdot)}{\partial d_{hn}} = tc \cdot X_{hn} - \frac{\partial U(\cdot)}{\partial A}\frac{\partial A}{\partial d_h n}. \tag{A6}
$$

Conditional on water quality c_n, this expression shows that households pay for (reduced) distance through one channel (home prices) for two reasons: to consume amenity services and to reduce the cost of accessing recreation services at the local waterbody. We are interested in the value of changes in water quality conditional on location and so this expression does not enter our damages calculations.

Finally, the first-order conditions for non-local trips are

$$
-\frac{\partial U(\cdot)}{\partial X_j} = tc \cdot d_{nj}, \, \forall j \neq n, \tag{A7}
$$

which give rise to $J-1$ demand equations for visits to the non-local waterbodies. Differentiating the utility maximization problem with respect to c_j for any $j \neq n$ leads to

$$
\frac{\partial U(\cdot)}{\partial X_j}\frac{\partial X_{hj}(\cdot)}{\partial c_j} - tc \cdot d_{nj} \cdot \frac{\partial X_{hj}(\cdot)}{\partial c_j}, \tag{A8}
$$

where $\frac{\partial X_{hj}(\cdot)}{\partial c_j}$ represents a behavioral response. We use the first-order condition in (A7) to write (A8) as

$$
\frac{\partial U(\cdot)}{\partial X_j}\frac{\partial X_{hj}(\cdot)}{\partial c_j} = tc \cdot d_{nj} \cdot \frac{\partial X_{hj}}{\partial c_j} \, \forall j \neq n. \tag{A9}
$$

In our simple model there is no behavioral condition related to the CWS tariff. We assume the water utility sets its tariff to recover costs and that a higher pollution level increases these costs, which are passed on to households. There are no health or drinking water quality effects in the model. With these simplifications, the CWS component in our model operates as a pure income effect. A decrease in source water quality Δc_n increases treatment costs, which are passed on as a tariff increase $\Delta \tau_n$.

Equations (A4), (A5), (A9), and assumptions on CWS cost passthrough provide the basis for our empirical measurement of local marginal damages from a change in water quality in the landscape, holding location fixed. Specifically,

$$\begin{aligned} \mathrm{MD}_{hn}(c_1, \ldots, c_J) &= \frac{\Delta\tau_n}{\Delta c_n} - \frac{\partial U(\cdot)}{\partial A}\frac{\partial A}{\partial c_n} - \sum_{j=1}^{J}\frac{\partial U(\cdot)}{\partial X_j}\frac{\partial X_{hj}}{\partial c_j} \\ &= -\frac{\partial P(\cdot)}{\partial c_n} - \sum_{j\neq n}\left(tc \cdot d_{nj} \cdot \frac{\partial X_{hj}(\cdot)}{\partial c_j}\right) - tc \cdot d_{hn} \cdot \frac{\partial X_{hn}(\cdot)}{\partial c_n} + \frac{\Delta\tau_n}{\Delta c_n}. \end{aligned} \tag{A10}$$

We estimate marginal damages by assembling empirical representations of the right-hand side terms in (A10).

B Hydrology

An important hydrological component of our IAM is built off the US Geological Survey's SPARROW model. The modeling framework is described in Smith et al. (1997) and Schwarz et al. (2006). Preston et al. (2009) provide a non-technical overview. SPRARROW is a hybrid model that combines physical and statistical elements to characterize the spatial distribution of nutrient pollution loading and ambient water quality outcomes. The focus is on long-term (steady state) averages based on hydrological features of the landscape, land use patterns, and major point and nonpoint sources of emissions. It abstracts from intra-annual variation in pollution outcomes that arise from idiosyncratic weather patterns, seasonal land use changes, and other short-term shocks. We use five regional SPARROW models that collectively represent the contiguous US to (a) quantify total nitrogen (TN) and total phosphorus (TP) emissions (loads) into watersheds; (b) characterize baseline concentrations of TN and TP across the landscape; and (c) estimate counterfactual changes in downstream concentrations from marginal changes in loading. In this Appendix we describe the SPARROW model and how we use the model structure for these tasks.

The SPARROW framework uses a river or lake segment and its catchment area – the surrounding land area that drains into the river segment – as the unit of analysis. River and lake segments and their catchments are identified from the National Hydrography Database (NHD) Plus V2 at a fine level of spatial resolution.[1] River and lake segments can represent sections of small streams with perennial or intermittent flow, large permanent rivers, or impoundments (lakes and reservoirs) and impoundment outlets. For modeling purposes, river and lake segments are defined as lines connecting upstream and downstream nodes (points). A river segment i is hydrologically connected to upstream and downstream segments. An adjacent upstream segment $i-1$ flows into segment i, while an adjacent downstream segment $i+1$ receives flow from segment i. The SPARROW model maintains an ordering of river and lake segments in the direction of flow from a headwater (a segment with no upstream adjacent segment) to a receiving water (a segment with no downstream adjacent segment). It enforces mass balance conditions so that the quantity of emissions released at a point in space is tracked throughout the stream network as the sum of losses during constituent transport downstream and loading into receiving waters.

[1] Throughout the paper, we describe most rivers, streams, and other waterbodies used to route pollution as river or lake "segments." In our hydrology data and models, these individual river, streams, and lake segments are known as "comids" and serve as unique identifiers in the data. Our routing program uses comids for rivers, streams, lakes, and other waterbodies to connect upstream areas to downstream areas. HydroEcon uses the NHDPlusV2 Medium Resolution Model, which is also the model that forms the river and stream network for the USGS SPARROW regional models.

The statistical component of SPARROW uses stream flow and pollution concentration data from a monitoring network to calibrate the relationship between pollution mass flowing through a river or lake segment and pollution sources and land use characteristics. An important pre-processing step uses the network of stream flow gauges and pollution monitors to predict long-term average stream flow (in cubic feet per second) and long-term average flux of TN and TP (in kg per year) leaving each segment in the model. SPARROW then uses nonlinear regression and a specific parametric relationship to estimate the parameters θ in the function

$$\mathrm{F}_i = g(F_{i-1}, S_{i1}, ..., S_{iN}, Z_i; \theta), \tag{B1}$$

where F_i is the flux of pollution (e.g., kg per year of TP) leaving segment i, F_{i-1} is the flux of pollution leaving the adjacent upstream segment (or segments), and S_{in} is one of N local pollution sources entering segment i from its catchment or being directly emitted into segment i. The term Z_i is a collection of variables describing the stream and landscape characteristics, including long run average flow, that affect delivery of pollution locally into the segment and the attenuation processes acting on flux as it travels along the segment pathway.

There are three features of the empirical SPARROW model that are important for HydroEcon. First, predictions at the segment level for long-term average flux of TN and TP and long-term average stream flow allow us to compute long term average baseline concentrations of TN and TP across the landscape. Second, S_{in} can represent directly observed emissions (e.g., point source emissions from wastewater treatment plants) or it can be a proxy for unobserved emissions (e.g., emissions from cropland acres in a catchment). Including both types of source variables allows the model to be relatively comprehensive in its coverage of major pollution sources. In addition, the functional form and parameter estimates allow F_i to be apportioned across contributions from the upstream flux and contributions from local pollution sources entering the segment. This in turn allows us to assign annual nutrient loads at the segment level for the major point and nonpoint sources of pollution.

Third, the empirical specification captures constituent loss from local sources S_{in} and upstream flux F_{i-1} as pollution mass travels along the stream network. River and lake segment specific variables such as stream flow, average temperatures, soil characteristics, conservation practices, and withdrawals for irrigation and other purposes determine the proportion of upstream flux and local loads that are passed to the downstream segment. This key SPARROW capability allows us to observe the local load of TN and TP entering

a river or lake segment (incremental yield into segment i) and the amount of the local load that is delivered to the receiving water (delivered yield from segment i).

We use the ratio of delivered yield to incremental yield to predict the changes in downstream concentrations that follow a marginal change in nutrient load. We define a delivery ratio $DR_i \leq 1$ as the proportion of the total local load of a nutrient (TN or TP) that is delivered to the receiving water. There is variation in delivery ratios across the landscape due to variation in landscape attributes and distance to the receiving water. In general, we expect delivery ratios to be smaller for distant upstream segments and larger for downstream segments that are near the receiving water. In practice this means that

$$DR_{i-1} \leq DR_i \leq DR_{i+1}, \tag{B2}$$

for upstream and downstream adjacent segments that are similar in their physical characteristics. We use this to define a segment-specific decay rate

$$decay_{i+1}^{i} = \frac{DR_{i+1} - DR_i}{DR_{i+1}}, \tag{B3}$$

If equation B2 holds, the decay rate will be a positive number in the unit interval.[2] It measures the proportion of incremental load to river or lake segment i that is lost on its way downstream to segment $i+1$.

We use the decay rates to predict downstream changes in concentration that follow from a place specific change in load. Define $\triangle L_i$ as an incremental addition to long term average load for a nutrient in segment i. The resulting change in long term average nutrient flux at downstream segment $i+k$ is

$$\triangle F_{i+k} = \triangle L_i \prod_{j=0}^{k-1} (1 - decay_{i+j+1}^{i+j}). \tag{B4}$$

For each downstream segment $i+k$ we compute the updated long term average flux as

[2]In our application, this restriction holds for over 98% of our river segments. In the rare instances where a delivery ratio in the i segment is less than the delivery ratio in the $i-1$ segment, we set it equal to the $i-1$ segment. We also assume no decay occurs in headwater streams.

$F_{i+k} + \triangle F_{i+k}$ and compute the updated nutrient concentration using the baseline long term average flow.

For our empirical implementation we use five regional SPARROW models that collectively represent the contiguous US. The models are the result of a major effort completed in 2019 that implemented state of the art SPARROW methodology and used monitoring data for stream flow and nutrient pollution concentrations collected between 2000 and 2014. The effort was completed in stages, with Saad et al. (2019) describing the preprocessing steps that were used to estimate long-term average stream flow and nutrient loads at monitoring sites across the country. Robertson and Saad (2019), Ator (2019), Wise (2019), Hoos and Roland II (2019), and Wise et al. (2019) then describe models for the Midwest, Northeast, Pacific, Southeast, and Southwest regions, respectively. We access results for each model from the USGS SPARROW Mapper website.[3] The output files provide river or lake segment specific predictions for long term average TN and TP flux, stream flow, incremental and delivered yield for TN and TP, and individual pollution sources.

Appendix Figure B.1 displays the spatial distribution of loads and concentrations for TN and TP at the watershed level. Watershed level loads are the sum of incremental (local) loads across all segments in the watershed. Concentrations are computed as the flow-weighted average of segment concentrations (calculated as the ratio of flux and stream flow) across all segments in a watershed. Unless stated otherwise, we winsorize concentrations at the 1st and 99th percentile within each SPARROW region. We adjust loads only for our marginal damage calculations, but do not winsorize them separately for GED estimates. Our marginal damages calculations rely on simulating changes in concentrations from a pulse in upstream loads. When we follow these loads downstream, we add the marginal change in loads to the river segment specific load to estimate changes in concentrations. For those river segments where we winsorize concentrations, we adjust the annual load estimate for that river segment to reflect the winsorized concentration.

Table B.1 provides summary statistics on the hydrologic network and corresponding water quality measurements for each of the five SPARROW models. For some measures, we report the corresponding statistics for NHDPlusV2, SPARROW, and HydroEcon since our model uses the NHDPlusV2 as its hydrological base and then links to SPARROW for information on decay, concentrations, and loads. The table shows that our model captures a high level of granularity - HydroEcon uses approximately 2.7 million river segments and each river segment is, on average, less than 2km in length. The Midwest SPARROW model comprises

[3]Online at https://www.usgs.gov/mission-areas/water-resources/science/sparrow-mappers.

the largest area, encompasses the most states, and accounts for approximately half of the river segments. HydroEcon uses most of the river segments in NHDPlusV2 and SPARROW; however, some river segments are dropped through the following process. First, we use the National Seamless Database from the NHDPlusV2 as our routing network. We keep only river segment pairs where the direction is defined as having a flowing connection between these pairs (this corresponds to direction value of 709 which is a flowing connection). This restriction excludes most coastal boundaries. We then exclude divergences from this list. This leaves us with 2,664,564 unique river segments as reported in Table B.1. HydroEcon uses all watersheds from NHDPlusV2 except one, HUC8 12110203. Nearly all river segments in this watershed are classified as coastal. The one exception, comid 1587295, crosses another HUC8 watershed, 12110205, and is primarily found within it. Thus, we assign comid 1587295 to this non-coastal watershed. We also report the TP and TN concentrations for the winsorized sample, as well as the full sample. Due to some extremely and unrealistically large outliers, especially in the Pacific and Midwest models, our winsorization process yields smaller average concentrations for TP and TN.

Table B.2 provides additional summary statistics for HydroEcon. First, we report the number of distinct lakes that are used within the recreation, housing, and climate change damages modules since these damage estimates are highly dependent on the presence and water quality of lakes. Our recreation and housing modules use approximately 17% of all lakes within the NHDPlusV2 and reflect those lakes that are larger than 0.1 km^2. Our climate change module includes many more smaller lakes, including all lakes greater than 0.01 km^2. This captures most (94%) the waterbodies designated as lakes within the NHDPlusV2. For purposes of reporting, when lakes overlap multiple states, we assign lakes to states based on the centroid of each lake.

In Table B.2, we also report the TP and TN loads by Census Region that correspond to loads reported in Table 3. These statistics show that the Midwest contributes the largest share of TP and TN loads, primarily due to agriculture's large contribution. However, municipal wastewater and urban non-point sources also contribute significant portions, especially in the South. For purposes of reporting of loads and GED, when watersheds overlap states, we assign watersheds to states based on the share of the watershed that is within a state.

Table B.1: Summary of Regional SPARROW Models

Category	Northeast	Southeast	Midwest	Southwest	Pacific	All
States	ME, NY, NJ, PA, MD, VA, VT, NH, DE, MA, RI, WV, CT, DC	AL, FL, GA, NC, SC, VA, TN, MS	CO, WY, MT, OK, MI, AR, TX, WV, KY, VA, OH, MO, IA, NE, KS, IL, NM, LA, MN, WI, TN, SD, ND, IN, PA, MD, NC, MS, NY, AL, GA	TX, ID, UT, NV, CO, AZ, NM, LA, CA, WY, OR	CA, OR, MT, ID, WA, WY, UT, NV	-
Avg. Length of River Segment (km)	1.52	1.46	1.91	2.56	1.88	1.93
No. of River Segments						
NHDPlusV2	197,332	323,647	1,378,929	440,497	342,453	2,689,508
SPARROW	197,576	323,770	1,379,904	440,985	342,454	2,684,689
HydroEcon	190,812	316,752	1,373,610	438,810	338,846	2,664,564
Number of HUC 8s						
NHDPlusV2	159	193	1,006	440	319	2,113
SPARROW	159	193	1,006	440	319	2,106
HydroEcon	159	193	1,006	439	319	2,112
Avg. TP Concentration						
Winsorized	0.073	0.117	0.329	0.153	0.169	0.235
Full Sample	0.08	0.125	4.396	0.255	$1.14 \cdot 10^{19}$	$1.47 \cdot 10^{18}$
Avg. TN Concentration						
Winsorized	1.126	1.101	2.332	0.705	1.051	1.665
Full Sample	1.236	1.108	2.598	0.741	$2.10 \cdot 10^{98}$	$2.67 \cdot 10^{97}$

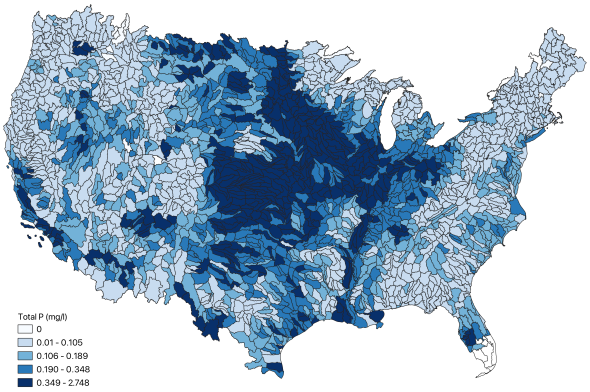
Notes: This table displays summary statistics for the NHD Plus V2, SPARROW, and HydroEcon across the five primary regional SPARROW models.

Table B.2: Summary of HydroEcon by Census Region

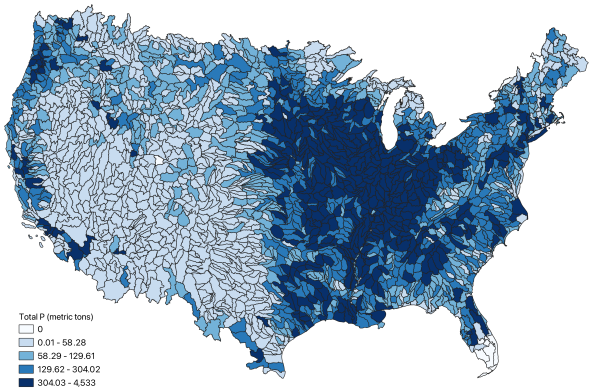
	Northeast	**South**	**Midwest**	**West**	**All**
No. of Lakes					
NHDPlusV2	27,695	140,641	150,629	60,112	379,077
Recreation ($> 0.1km^2$)	6,899	20,655	27,072	10,012	64,638
Housing ($> 0.1km^2$)	4,826	10,150	14,372	2,249	31,597
Climate Change ($> 0.01km^2$)	25,385	133,032	142,285	55,284	355,986
TP Loads (thousand metric tons/yr)					
Non-point Sources					
Agriculture	6.1	74.3	106.2	13.8	200.4
Urban	4.0	17.5	13.3	2.5	37.3
Point Sources					
Municipal Wastewater	10.5	21.1	20.7	13.1	65.3
Other	7.2	46.7	33.4	23.3	110.7
TP Loads per Year	27.8	159.6	173.6	52.7	413.7
TN Loads (thousand metric tons/yr)					
Non-point Sources					
Agriculture	97.1	348.0	1,097.4	89.0	1,631.5
Urban	29.6	41.5	30.0	17.4	118.6
Point Sources					
Municipal Wastewater	50.4	130.8	77.2	52.1	310.5
Other	162.1	471.1	490.7	165.8	1,289.6
TN Loads per Year	339.2	991.4	1,695.3	324.3	3,350.2

Notes: This table displays summary statistics for the NHD Plus V2 and HydroEcon across Census Regions. Other sources of phosphorus loads include natural sources, emissions from Canada, mineral erosion, mining, inter-basin transfer, channel erosion, and spring discharge. Other sources of nitrogen loads include emissions from Canada, septic systems, spring discharge, channel erosion, scrub and grasslands, and red alder trees.

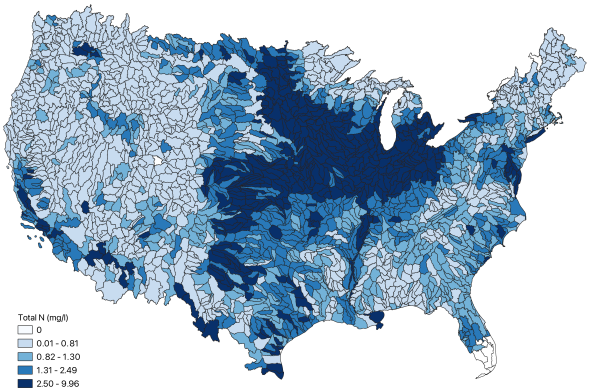
Figure B.1: Baseline Total Phosphorus and Total Nitrogen Concentrations and Loads



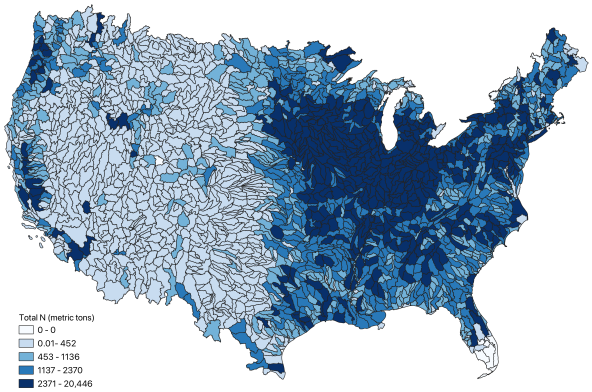
(a) Total Phosphorus Concentration (mg/l)



(b) Total Phosphorus Loads (metric tons/yr)



(c) Total Nitrogen Concentration (mg/l)



(d) Total Nitrogen Loads (metric tons/yr)

Notes: This figure displays baseline, long-run annual average concentrations and loads of Total Phosphorus (Panels A and B) and Total Nitrogen (Panels C and D) by watershed. Darker shades of red represent higher concentrations and greater loads. Watersheds where concentrations or loads are not estimated are displayed as white.

C Damage Modules

C.1 Recreation

Our recreation module provides an empirical representation of the recreation component of total marginal damage from a pulse in upstream nutrient load, given in equation 3 by:

$$\triangle RV = -\sum_{h=1}^{H}\sum_{j=1}^{J}\frac{\partial U}{\partial X_j}\frac{\partial X_{hj}(c_j)}{\partial c_j}\triangle c_j, \tag{C1}$$

where j indexes lakes, X_{hj} is trips by person h to lake j, c_j is the nutrient concentration in lake j, and $\frac{\partial U}{\partial X_j}$ is the value of a recreation trip. Specifically, the module predicts the landscape wide economic damage from changes in total phosphorus concentration in lakes, which arise from an upstream change in phosphorus emissions. The key empirical components include a dose-response function relating a change in individual water recreation trip taking to a change in total phosphorus, the value of a lost recreation day, and the baseline and changed levels of total phosphorus concentration in lakes larger than 0.1km^2.

For the dose response function, we define $h = ct$ as a representative person in census tract ct and J_{ct} as the subset of lakes larger than 0.1km^2 in the landscape that are within 100 miles of the center of tract ct. Furthermore, we define

$$X_{ct}(WQ_{ct}) = \sum_{j=1}^{J_{ct}} X_{ct,j}(c_j), \tag{C2}$$

where WQ_{ct} is the weighted average of nutrient concentrations among the J_{ct} lakes given in equation 5.

We calibrate $X_{ct}(WQ_{ct})$ using parameter values from Keiser (2019), who estimates the causal relationship between freshwater recreation trip taking and total phosphorus concentrations in lakes across the US. The study uses annual trips for over 29,000 individuals who participated in the National Survey of Recreation and the Environment (USDA, 2009) between 1999 and 2009. Survey data on trips for swimming, fishing, boating, and visits to noncoastal watersides for other activities are used to compute annual days of water recreation for each person in the sample. The paper computes home county-level average phosphorus concentrations using data collected at 1,208 lakes during summer 2007 as part

of the US EPA National Lakes Assessment (USEPA, 2007). The NLA lake sampling plan is designed to provide representative water quality levels in lakes across the country, which allows Keiser (2019) to assign average lake water quality for 1,846 counties in 41 states across the continental US[1]. Using a semi-log functional form, the study regresses individual trip counts on home county average phosphorus concentration while controlling for individual socio-economic characteristics, county level geospatial variables, and state-level fixed effects. Keiser (2019) implements an instrumental variable approach to identification whereby water quality in places that are hydrologically upstream is an instrument for local water quality.

We use estimates from Keiser (2019), table 2, panel A, column 2 to calibrate equation C2 based on the functional form in equation 6. The vector Z_{ct} matches Keiser (2019)'s specification and includes socio-economic (race, gender, age, income, education) and geospatial (metropolitan area dummy, coastal area dummy, average temperature, average precipitation, elevation, predominant land cover type, lake presence dummy) variables and state fixed effects. We assign socio-economic values using the census tract average and follow Keiser (2019) by assigning geospatial values at the county level.

Keiser (2019) does not include CA, NV, NM, AZ, UT, WY, and CO in his application due to data limitations. As a result, his model includes 40 non-zero state fixed effects plus one additional state fixed effect normalized to zero. We include the seven omitted states in our model by imputing their fixed effects via a boundary rule. In practice this means we assign the fixed effect from Oregon to CA and NV, from Texas for NM and AZ, from Idaho for UW and WY, and from Kansas for CO.

The parameter on water quality is $\beta_{wq} = -3.405$. The average total phosphorus concentration in Keiser (2019) is 0.061 mg/l (see table 1 in the study), implying an elasticity of trips with respect to pollution in his application of -0.207. This elasticity and our spatially varying prediction for baseline trips are the basis for our dose response function:

$$\triangle X_{ct} = exp(\beta_0 + \beta_1 Z_{ct})[exp(\beta_{WQ} WQ^0_{ct}) - exp(\beta_{WQ} WQ^1_{ct})], \tag{C3}$$

where 0 and 1 denote the baseline and counterfactual levels of total phosphorus pollution assigned to census tract ct.

To value a lost recreation day, we use $RDV = \$70$ in 2016 dollars based on the College of Forestry, Oregon State University (2010). This database combines 3,129 estimates from

[1]Counties that do not have a lake included in the 2007 NLA sample are assigned the water quality value for a neighboring county.

421 documents on the use value of recreation activities in the US and Canada spanning the period 1958-2015. The database provides estimates of net willingness to pay or consumer surplus in per person-day units for 21 primary recreation activities, differentiated by broad geographic scale. All values are adjusted to 2016 USD. To construct our RDV we selected studies from the database that analyzed freshwater fishing, nonmotorized boating, motorized boating, swimming, and general recreation. Our average of \$70.09 (rounded to \$70) is based on XX individual study estimates.

For census tract demographic variables, we use the five-year averages reported in the 2017 American Community Survey (ACS). This includes the census tract level adult population, pop_{ct}, which we use to construct our estimate of the damages from a change in total phosphorus concentration according to

$$\triangle RV = RDV \cdot \sum_{ct=1}^{C} \triangle RV_{ct} \cdot pop_{ct}, \tag{C4}$$

where C is the number of census tracts in the continental US.

A summary of our calibration decisions for the recreation module is included in table X.

C.2 Hedonics

Our property value module provides an empirical representation of the amenity component of total marginal damage from a pulse in upstream nutrient load, given in equation 3 by:

$$\triangle HV = -\sum_{n=1}^{N}\sum_{h=1}^{H_n}\frac{\partial U}{\partial A}\frac{\partial A(d_{hn}, c_n)}{\partial c_n}\triangle c_n \tag{C5}$$

where n indexes neighborhoods, H_n is the number of households in neighborhood n affected by the amenity change, c_n is the nutrient concentration in the local waterbody, and the utility terms denote the marginal willingness to pay by household h for a change in amenity services operating through a change in local water quality. Equation A5 shows that, in equilibrium, the marginal willingness to pay is equal to the hedonic price gradient:

$$\frac{\partial U}{\partial A}\frac{\partial A(d_{hn}, c_n)}{\partial c_n} = \frac{\partial P(\cdot)}{\partial c_n} \tag{C6}$$

To compute equation C6, we use estimates from Mamun et al. (2023) to measure the relationship between home prices and water clarity for properties near inland lakes. Information on the universe of nearshore residential properties from the Core Logic assessment database is used to compute H_n and to aggregate the damages. We use data from the US EPA National Lakes Assessment (US EPA 2009, 2016) to relate changes in ambient nutrient concentrations to changes in water clarity. Finally, we use estimates from Bishop et al. (2025) to convert changes in asset values to annual damages. Details on each of these steps are given in this Appendix section.

Mamun et al. (2023) conducted a national-scale hedonic property analysis to measure the relationship between home values and water quality in inland lakes in the continental US. They assemble water quality data on over 1,600 freshwater lakes from the US EPA Water Quality Portal and the LAGOS-NE database (Soranno et al., 2017). Data on water clarity (measured as Secchi depth) are matched to residential home sales drawn from the Zillow ZTRAX database, occurring between 2000 and 2019 and within 2km of freshwater lakes. The estimation sample includes nearly 750,000 sales. Identification relies on a fixed effects design that exploits within-lake variation in water quality over time. Mamun et al. (2023) find that a 1 percent increase in water clarity leads to a $\eta_1 = 0.18$ percent increase in sale price for properties within 100m of the lakeshore. For properties between 100m and 300m from shore, a 1 percent increase in clarity increases price by $\eta_1 = 0.04$ percent.

We use the Core Logic Basic Property assessment database to inventory single-family residential homes that are within 300m of inland lakes larger than 0.1km^2. We begin by selecting the most recent assessment for single-family residential homes in the continental US that occurred in the 2017-2021 window. This generated 92.13 million unique records with valid location and assessed values. We matched these properties to their nearest inland lake larger than 0.1km^2. There were 45,335 lakes with properties closer than 3km from shore. We then identified properties with distances equal to or smaller than 300m to the nearest lake. This resulted in 3.51 million homes near 31,597 lakes. The total assessed value for these properties is \$961.41 billion (2021 dollars). This divides out as V^1 = \$378.85 billion for homes closer than 100m from shore and V^2 = \$582.55 billion for homes in the 100m to 300m distance bin.

To measure amenity damages from nutrient pollution, we need to translate changes in nutrient concentration into changes in Secchi depth (water clarity). We use data from the 2007 and 2012 National Lake Assessments (NLA; US EPA 2009, 2016) for this. The 2007 NLA selected 1,028 lakes that are representative of 50,000 natural and manmade lakes that are greater than 10 acres. The 2012 NLA selected 1,038 lakes that are representative of 110,000 natural and manmade lakes that are greater than 2.5 acres. A range of water quality parameters was measured for each lake in the two cross-sections, including Secchi depth and total phosphorus concentrations. For some lakes, multiple measurements were taken at different times during the sample year. To quantify the relationship between Secchi depth and total phosphorus, we pool the two cross-sections and use a log-log specification given by:

$$ln(SD_{ij}) = v_{0r} + v_r ln(TP_{ij}) + \epsilon_{ij} \tag{C7}$$

where SD_{ij} is measure i of Secchi depth at lake j and TP_{ij} is total phosphorus concentration. The key parameter is v_r, which measures the percentage change in Secchi depth from a 1 percent change in total phosphorus. We estimate nine values of this parameter, each corresponding to an ecological region. The parameter estimates range from 0.39 to 0.50.

Finally, we use findings from Bishop et al. (2025) to select an annualization rate for translating a change in asset value into an annual measure. Bishop et al. (2025) estimate the time and space-varying annual cost of homeownership and express this cost as a proportion of the asset value, labeled the user cost rate. In their analysis, the user cost rate for a given homeowner depends on variables like the loan-to-value ratio, the rate of return on capital, the mortgage rate, property taxes, the rate of depreciation, expected capital gains, and features

of the tax code. Bishop et al. (2025) assemble data and perform analysis to compute the user cost rates for the years 2012 to 2019 for all Public Use Microdata Areas (PUMAs) in the US. We use the nationwide average user cost rate for 2019 of $\alpha = 0.0448$ for our model.

These data components allow us to compute the amenity mechanism damages from a change in nutrient concentration in downstream river segments following an emissions pulse. We focus on damages from changes in phosphorus concentration. Denote $\triangle c_j$ as the change in phosphorus concentration at a lake j that is affected by an upstream change in load. The damages from the set of lakes J_k that are affected by the load change is:

$$\triangle HV = \sum_{j=1}^{J_k} \alpha \cdot \frac{(V_j^1 \cdot \eta_1 + V_j^2 \cdot \eta_2)}{100} \cdot v \cdot \%\triangle c_j, \tag{C8}$$

where α, η_1, η_2, and v are defined above, V_j^1 is the total assessed value of homes within 100m of lake j, and V_j^2 is the total assessed value of homes in the 100m to 300m distance band of lake j. We assign the baseline phosphorus concentration for lake j to be equal to the average concentration in the watershed (HUC8) it is contained in. Likewise, the new concentration for lake j following an upstream pulse is assigned based on the new watershed average concentration.

A summary of the parameter assignments used in the property value module is included in Table X.